

OPTIMAL SIZING AND DISPATCH OF COOLING SYSTEMS WITH COLD
THERMAL ENERGY STORAGE FOR COMMERCIAL BUILDINGS:
A MIXED-INTEGER NONLINEAR PROGRAMMING APPROACH

by

Raido Huberg

Copyright by Raido Huberg 2013

All Rights Reserved

A thesis submitted to the Faculty and the Board of Trustees of the Colorado School of Mines in partial fulfillment of the requirements for the degree of Master of Science (Engineering).

Golden, Colorado

Date _____

Signed: _____

Raido Huberg

Signed: _____

Dr. Robert Braun

Thesis Advisor

Golden, Colorado

Date _____

Signed: _____

Dr. Greg Jackson

Department Head

Department of Mechanical Engineering

ABSTRACT

Commercial buildings account for a large fraction of electricity consumption in the United States. Literature indicates that distributed multi-energy systems have the potential to reduce the annual cost and emissions and to improve the energy conversion efficiency of a commercial building energy system. In addition, thermal energy storage has been found to improve the energy efficiency, reduce emission rates and improve the economics of a building energy system. In the literature, numerous prime movers, system configurations and dispatch strategies have been investigated. Solid oxide fuel cell (SOFC) technology promises high-efficiency and low emission conversion of readily available natural gas, compared to conventional technologies like Stirling engines and micro-turbines; thus, SOFCs have garnered significant interest as prime movers. However, the design and dispatch of distributed multi-energy generation systems in the presence of cooling, heating and power demand, along with time-of-use utility pricing and/or demand charges for a full year, is a complex endeavor and there is a lack of understanding of how to design, size and dispatch such a system.

A previously developed method by Pruitt et al., 2012 is used to solve linear approximations of mixed-integer non-linear programming models. The previously developed method is capable of finding the design of the system, the size of different DG technologies, and dispatch strategy for a distributed multi-energy generation system meeting the energy needs of a building at a minimum annual cost. Technologies and energy systems investigated in this study are: power-only, co-generation of heat and power (CHP) and co-generation of cooling, heat and power (CCHP) SOFCs (with variable efficiency and minimum turn-down ratios), cold water storage tanks, and absorption and vapor compression chillers. In addition, we investigate the effects of both time-of-use and demand charges for electric power consumption. Our optimization efforts reveal that Cold Water Storage (CWS) tanks have great savings potential in today's market conditions, compared to absorption chillers. CWS tanks reduce the total annual costs by up to 16% and result in a negative payback time and reduced carbon dioxide emissions by 1.5 to 4% for all cases considered, by increasing the COP of chillers. In addition, we present sensitivity analysis on several technology characteristics and on the utility pricing.

TABLE OF CONTENTS

ABSTRACT.....	iii
LIST OF FIGURES	vii
LIST OF TABLES	viii
NOMENCLATURE	ix
LIST OF ABBREVIATIONS.....	xiv
ACKNOWLEDGEMENTS	xvi
CHAPTER 1 INTRODUCTION	1
1.1 Motivations	1
1.2 Problem Statement	4
1.3 Research Objectives.....	4
1.4 Thesis Overview	5
CHAPTER 2 LITERATURE REVIEW AND APPROACHES	9
2.1 Approaches and Modeling Tools	9
2.2 Literature Review.....	11
2.3 Conclusions drawn from the literature review	14
CHAPTER 3 CCHP SYSTEM COMPONENTS AND INPUT DATA	18
3.1 CCHP System	18
3.1.1 Solid Oxide Fuel Cell Systems.....	21
3.1.2 Cold Thermal Storage	23
3.1.3 Vapor Compression Chillers	24
3.1.4 Absorption Chillers	25
3.2 Chiller COP values	27
3.2.1 Absorption Chiller COP	28
3.2.2 Vapor Compression Chiller (VCC) COP	29
3.2.3 COP analysis (VCC and absorption chiller).....	30
3.3 Building Types and Locations	33
3.3.1 San Francisco	35
3.3.1.1 Load profiles	35
3.3.1.2 Utility	37

3.3.2	Boston.....	38
3.3.2.1	Load profiles	38
3.3.2.2	Utility	38
3.3.3	CO ₂ emission rate from natural gas.....	39
3.4	Summary of Input Data.....	40
3.5	Assumptions.....	40
CHAPTER 4	MODEL.....	43
4.1	Distributed CCHP Generation System.....	43
4.2	System Technologies	44
4.3	Model Description	44
4.4	Mathematical Formulation P	46
4.4.1	Minimum Total Cost	46
4.4.2	Power, Cooling and Heating Demand.....	49
4.4.3	Utility Restrictions	50
4.4.4	Power and Cooling Capacity.....	50
4.4.5	Electric Efficiency.....	50
4.4.6	Natural Gas and Power Consumption	51
4.4.7	Start-Up and Ramping of SOFC(-CHP)s	51
4.4.8	Heat Capacity	52
4.4.9	Cold Thermal Storage	53
4.4.10	Non-negativity and integrality.....	54
4.5	Solution techniques.....	54
4.5.1	Mathematical Structure	55
4.5.1.1	Lower Bounding: Convex Underestimation U	55
4.5.1.2	Upper Bounding: Linearization Heuristic H.....	57
4.6	Summary of optimization runs.....	58
CHAPTER 5	RESULTS AND DISCUSSION.....	59
5.1	Existing Building Energy System.....	59
5.2	Simple payback time (SPT)	61
5.3	Effects of chiller COP	61
5.4	Switch Points and Sensitivity Analysis	63
5.4.1	Absorption chillers	63

5.4.2	Tax on carbon dioxide emissions	63
5.5	Addition of an Absorption Chiller	64
5.5.1	Dispatch for VCC and absorption chiller system	66
5.6	Addition of Chilled Water Storage (CWS) Tank.....	68
5.6.1	Dispatch for a CWS tank.....	70
5.7	Summary of Results	73
CHAPTER 6 CONCLUSIONS		74
6.1	Major Findings.....	74
6.1.1	Effect of DER technology efficiency performance	74
6.1.2	Effect of cold thermal storage	75
6.1.3	Effect of system configuration	75
6.2	Future Work	75
REFERENCES CITED.....		77

LIST OF FIGURES

Figure 1-1: Breakdown of U.S. Electricity Consumption.....	2
Figure 3-1: CCHP system flow diagram with CWS.....	19
Figure 3-2: SOFC with direct internal reforming [18].....	22
Figure 3-3: Stratified CWS tank [7].....	24
Figure 3-4: Vapor compression chiller	25
Figure 3-5: Double-effect absorption chiller [65].....	27
Figure 3-6: Part load operation, double-effect absorption chiller [6]	29
Figure 3-7: COP, double-effect absorption chiller	30
Figure 3-8: Cooling tower performance – 100% design flow [8].....	31
Figure 3-9: COP of VCC [66].....	31
Figure 3-10: Building Energy Load profiles in San Francisco, CA	36
Figure 3-11: Monthly energy consumption in San Francisco, CA	37
Figure 3-12: Monthly energy consumption in Boston, MA	41
Figure 3-13: Building energy load profiles in Boston	42
Figure 4-1: CCHP system diagram	44
Figure 5-1: Breakdown of total annual cost by end use.....	60
Figure 5-2: Breakdown of total annual cost by cost type	60
Figure 5-3: Cost breakdown comparison (VCC vs. VCC+ABS)	66
Figure 5-4: Chiller operation between VCC and VCC+ABS systems	67
Figure 5-5: Chiller operation (VCC vs. VCC+ABS).....	67
Figure 5-6: Cost breakdown (VCC vs. VCC+CWS).....	69
Figure 5-7: Chiller operation between (VCC vs. VCC+CWS)	70
Figure 5-8: Chiller operation (VCC vs. VCC+CWS).....	71
Figure 5-9: Two-day power needs profile of a large hotel in Boston.....	71
Figure 5-10: Share of VCC electricity the monthly peaks.....	72
Figure 5-11: Two-day power needs profile of a large hotel in San Francisco.....	73

LIST OF TABLES

Table 2-1: Summary of literature review.....	17
Table 3-1: COP _{min} and COP _{max} of chillers.....	32
Table 3-2: Adjusted COP values for VCC.....	32
Table 3-3: COP of VCC with and without CWS.....	33
Table 3-4: Random variability of power demand in San Francisco, CA.....	34
Table 3-5: Thermal-to-electric ratios.....	34
Table 3-6: Utility rates in San Francisco A-10, CA [52][53].....	39
Table 3-7: Utility rates in Boston, MA [40].....	40
Table 3-8: Summary of technology input parameters.....	42
Table 4-1: SOFC waste heat utilization matrix.....	53
Table 4-2: Summary of optimization runs.....	57
Table 5-1: Effects of changing the COP of VCC by $\pm 25\%$ on total annual cost.....	62
Table 5-2: % reduction in total installed cost required for the absorption chiller.....	63
Table 5-3: Sensitivity analysis of CO ₂ tax in Boston.....	64
Table 5-4: Installation of absorption chillers.....	65
Table 5-5: Installation of a CWS tank.....	68
Table 5-6: Summary of results.....	73

NOMENCLATURE

The sets, parameters, and variables referenced throughout the document are listed below, alphabetically. Upper-case letters identify variables or sets, while lower-case letters identify parameters or set indices. Superscripts and accents differentiate parameters and variables that use the same base letter. Subscripts distinguish between elements of a set. Some parameters and variables, which are identified in a given problem formulation, are only defined for certain elements of sets. The units of each parameter and variable are provided in brackets after its definition [47]

Sets

$i \in \mathcal{I}$ set of all cost elements

$j \in \mathcal{J}$ set of all technologies

$n \in \mathcal{N}$ set of all months

$t \in \mathcal{T}_n$ set of all hours in month n

$t \in \mathcal{T}$ set of all hours ($\mathcal{T} = \cup_n \mathcal{T}_n$)

Parameters

α_j average ambient heat loss of water stored in each technology j [fraction]

β factor converting from kJ to kWh [$3600 \frac{kJ}{kWh}$]

γ_j average exhaust output from each technology j per natural gas input [kg/kWh]

δ demand time increment [hours]

ε	an arbitrary small positive quantity
η_j^{\max}	maximum electric efficiency of each technology j [fraction]
η_j^{\min}	minimum electric efficiency of each technology j [fraction]
η_j^P	rated electric efficiency of each technology j [fraction]
η_j^Q	rated thermal efficiency of each technology j [fraction]
κ_j	initial capital cost of technology j [\$/kWh, \$/kW, \$/gal, or \$/m ³]
λ_j	average lifetime of technology j [number of time periods]
μ_j	minimum turn-down of each technology j [fraction]
ν_t	net-metering rate paid by utility for exported power in hour t [fraction]
ρ	interest rate [% (fraction) per time horizon]
σ_j	start-up time for each technology j to reach operating temperatures [hours]
τ_a	temperature of return chilled water [°C]
τ_b	temperature of supply chilled water [°C]
τ_j^{in}	average temperature of fluid into each technology j [°C]
τ_j^{out}	average temperature of fluid out of each technology j [°C]
τ^{\max}	maximum temperature of water in the system [°C]
τ^{\min}	minimum temperature of water in the system [°C]
$\Delta\tau_t^{\text{wb}}$	wet bulb temperature degrees above 0°C [°C]

b_j	fraction of annual O&M cost from the purchase cost of technology j [fraction]
b^{CHP}	binary for switching exhaust flow from SOFC to boiler [binary]
b^{CCP}	binary for switching exhaust flow from SOFC to chiller [binary]
b^{CCHP}	binary for switching exhaust flow from SOFC to chiller and boiler [binary]
$b^{CCHP,2}$	binary for switching exhaust flow from chiller to boiler [binary]
c_j	amortized capital and install cost of each technology j [\$/kWh, \$/kW, or \$/gal, \$/m ³]
c^p	specific heat of water [kJ/kg-°C]
cop_j^{\min}	minimum COP of technology j [kJ/kg-°C]
cop_j^{\max}	maximum COP of technology j [-]
Δcop_j^{\min}	change of cop_j^{\min} of each technology j with temperature [$\frac{1}{K}$]
Δcop_j^{\max}	change of cop_j^{\max} of each technology j with temperature [$\frac{1}{K}$]
d_t^P	average power demand of building in hour t [kW]
d_t^Q	average heating demand of building in hour t [kW]
d_t^C	average cooling demand of building in hour t [kW]
g_t	price of natural gas from the utility in hour t [\$/kWh]
h_j	specific heat of fluid output from each technology j [kWh/(kg °C)]
k_j^{out}	nameplate power rating out of each technology j [kW]
m_j	average O&M cost of each technology j [\$/kWh]

p_t	price of power from the utility in hour t [\$/kWh]
p_n^{\max}	peak demand charge for power from the utility in month n [\$/kW/month]
r_j^{down}	maximum ramp-down rate of each technology j [kW/hr]
r_j^{up}	maximum ramp-up rate of each technology j [kW/hr]
z	tax on carbon emissions [\$/kg]
z^g	average carbon emissions rate for natural gas combustion [kg/kWh]
z^p	average carbon emissions rate for utility power [kWh]

Variables

A_j	number of each technology j acquired [integer]
C_i	total cost of element i over time horizon of length $ \mathcal{T} $ [\$]
COP_{jt}	COP of each technology j operating in hour t [-]
E_{jt}	electric efficiency of each technology j operating in hour t [fraction]
F_{jt}^{in}	flow rate of exhaust gas into each technology j in hour t [kg/hr]
F_{jt}^{out}	flow rate of exhaust gas out of each technology j in hour t [gal/hr]
G_{jt}	aggregate natural gas input to each technology j in hour t [kW]
\dot{M}_t^{C}	mass flow-rate of cool water through the building at time t [kg/hr]
\dot{M}_t^{Q}	mass flow-rate of hot water through the building at time t [kg/hr]
\dot{M}_{jt}^{C}	mass flow-rate of cool water through technology j [kg/hr]

M_t^{tank}	mass of chilled water under the thermocline in hour t [kg]
\bar{M}^{tank}	maximum mass of chilled water under the thermocline [kg]
N_{jt}	number of each technology j operating in hour t [integer]
\hat{N}_{jt}	increased number of each technology j operating from hour $t - 1$ to t [integer]
P_{jt}^{in}	aggregate power input to each technology j in hour t [kW]
$P_{jt}^{\text{in,aux}}$	aggregate auxiliary power input to each technology j in hour t [kW]
P_{jt}^{out}	aggregate power output from each technology j in hour t [kW]
Q_{jt}	aggregate thermal energy stored in each technology j at the start of hour t [kWh]
Q_{jt}^{in}	aggregate heat input to each technology j in hour t [kW]
Q_{jt}^{out}	aggregate heat and/or cooling output from each technology j in hour t [kW]
ΔQ_t^{out}	net heat flow into the CWS tank in hour t [kW]
T_{jt}	temperature of water stored in each technology j in hour t [$^{\circ}\text{C}$]
U_t^{out}	power purchased from the utility in hour t [kW]
U_n^{max}	peak power purchased from the utility in month n [kW]
V_j	water storage capacity of technology j [gallons]
\bar{V}^{tank}	maximum volume of chilled water under the thermocline [m^3]

LIST OF ABBREVIATIONS

California Independent System Operator	CAISO
Combined Heat and Power	CHP
Co-production of Cooling, Heat and Power	CCHP
Coefficient of Performance	COP
Distributed Energy Resources Customer Adoption Model	DER-CAM
Distributed Generation	DG
Direct Current	DC
Department of Energy	DOE
Evolutionary Algorithm	EA
Energy Information Administration	EIA
Genetic Algorithm	GA
Greenhouse Gas Emissions	GGE
Higher Heating Value	HHV
Hybrid Optimization Model for Electric Renewables	HOMER
Internal Combustion engine	IC engine
Lawrence Berkeley National Laboratory	LBNL
Linear Program	LP
Molten Carbonate Fuel Cell	MCFC
Mixed-Integer Linear Program	MILP
Mixed-Integer Nonlinear Program	MINLP
Nonlinear Program	NLP
Network for New Energy Choices	NNEC

National Renewable Energy Laboratory

NREL

Photovoltaic

PV

Solid-Oxide Fuel Cell

SOFC

ACKNOWLEDGEMENTS

Many people have helped me on my path to complete this thesis. Without them I would not have been able to complete this work.

First, I would like to thank my advisor Dr. Robert J. Braun for his support and advice throughout my time at the Colorado School of Mines. Without his guidance and patience I would not have been able to make it happen. Secondly, I would like to thank Dr. Alexandra M. Newman for her support and guidance in helping me to understand the world of Operations Research. I would also like to thank Dr. Kristopher A. Pruitt, who developed the optimization methods used in this thesis and who also patiently explained how these methods work, allowing me to use them for the purposes of my thesis.

I would like to thank my friends and family, especially my girlfriend Katherine E. Doolittle, who have supported me throughout my academic efforts.

In addition to the above-mentioned people, I would like to thank Gavin H. Goodall, who helped me with both the write-up of this thesis and the optimization model used in this thesis.

CHAPTER 1

INTRODUCTION

Close to 99% of electric power in the United States is generated in centralized (central) power plants and only around 1% of electric power is generated in distributed generation power plants. Typically, centralized power generation occurs by converting a fossil-based, nuclear, or hydropower energy source to electrical power. Distributed power generation commonly involves converting fossil-based, small hydropower, or renewable energy sources (such as solar radiation, wind power and biofuels) to electricity. Central power plants are remotely located relative to the consumer and produce power in the 500 to 1000 MW range. Distributed power generation plants, on the other hand, can be below the megawatt scale and located relatively close to the consumer. Centralized power generation enjoys the benefit of economies of scale due to the size of central power plants. However, centralized power plants typically have numerous drawbacks given their scale and remoteness from the consumer. They are often plagued by significant grid losses due to the transmission and distribution of electric power over long distances, concentrated air pollution, and lost thermal (waste heat) energy, which leads to low power conversion efficiency. Distributed generation plants can tackle the drawbacks of centralized power generation, such as grid losses and concentrated air pollution. Additionally, the proximity to the consumer enables increased power conversion efficiencies through waste heat utilization. Therefore, it is not surprising that distributed generation is gaining interest as an alternative to centralized power generation.

1.1 Motivations

Primary energy in the US is consumed by four main sectors; those sectors are residential, commercial, industrial and transportation. Building operations contribute the most to the energy consumption of the commercial and residential sectors. The commercial and residential sectors only account for 41% of the total primary energy consumption in the US; however, their share is increasing compared with the industrial and transportation sectors. The increase of primary

energy in the building sector correlates well with the present and predicted future electricity consumption demands of the residential and commercial building sectors. According to the U.S. Department of Energy [12], approximately 74% of electricity in the US is consumed in commercial and residential buildings (Figure 1-1); and as primary energy consumption increases in these sectors, the electricity consumption is also increasing due to this trend.

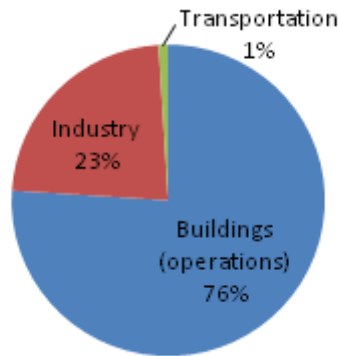


Figure 1-1: Breakdown of U.S. Electricity Consumption

Distributed generation (DG) does not enjoy the benefits of economies of scale that centralized power generation does; however, there are several factors that make DG an attractive alternative to centralized power generation. First, the electric utility industry has experienced extensive deregulation in order to simplify taking part in the power market. As a result of this deregulation, power generation and the power transmission distribution have been separated from one another. DG benefits from the separation of different sections of the power industry as consumers have the opportunity to choose a power generator. Power conversion in large power plants is relatively inefficient (~33% for large coal fired power plants). A byproduct of power conversion in fossil fuelled power plants is waste heat. When waste heat can be used for either cooling or heating purposes, the overall efficiency of the power plant is increased up to 80% according to Onovwiona et al. [42]. As a general rule, central power plants are remotely located, which severely limits the potential of utilizing waste heat from the power conversion in central power plants. Pecas-Lopes et al., [44] and Tan et al., [55] say that DG technologies are located closer to the consumer, allowing for a significant increase in the overall efficiency of the power plant. An energy system in which the waste heat of an electric power generating prime mover is utilized for heating is called combined heat and power (CHP). Waste heat can also be used for combined cooling and power (CCP) and combined cooling, heating and power (CCHP).

According to [23] combined generation or multi-energy generation systems (CHP, CCP and CCHP) will create the highest economic impact and likelihood of market adoption for distributed generation.

CHP, CCP and CCHP systems require a prime mover that produces electric power and waste heat. There are a number of different technology choices for prime movers, including internal combustion engines, Stirling engines, micro turbines and high temperature fuel cells. Fuel cell technology is in a pre-commercial state, making it more expensive per kW of installed capacity compared to other, conventional prime movers. However, characteristics such as a higher electrical efficiency (~45%) and reduced emissions make fuel cells a promising choice as a prime mover. High-temperature fuel cells, such as solid oxide fuel cells (SOFC) and molten carbonate fuel cells (MCFC), can use natural gas from the utility as fuel. Advanced exploration methods have made natural gas an abundant, relatively clean and cheap energy resource. A readily available infrastructure exists for natural gas supply. Fuel cells have been developed for basically any power source application: transportation, space exploration, portable energy and stationary power. The fuel cell industry has targeted the commercial building market in particular. This market creates the opportunity to take advantage of economies of scale by using DG technologies to utilize waste heat efficiently for space heating and/or cooling. Widespread adoption is elusive because power from the utility is relatively cheap, DG technology is generally expensive, and there is a lack of knowledge in design and dispatch of DG technologies and systems. For the above reasons, DG fuel cells, and DG in general, cannot often compete with central power plants.

With the potential increase of both primary and electric energy consumption in the building sector, the impact on the environment will increase. Concerns about harmful environmental impacts of power generation have prompted government to motivate the power industry to install environmentally benign power generation technologies and energy systems and to improve the performance of currently installed energy systems. Carbon taxing, attractive sellback rates and subsidizing the installation of environmentally benign technologies and energy systems has been applied in many regions and countries in the world [13]. Distributed multi-energy generation systems offer significant increase in power conversion efficiency. Because of the high conversion efficiencies, distributed multi-energy generation systems find support from the legislature [56] through deregulation. The increasing frequency of extreme weather

conditions has added focus to climate change and the necessity to use resources in an efficient way. High efficiency energy systems, like CHP and CCHP, are vital in tackling the environmental issues the world is facing.

1.2 Problem Statement

In this study, we are investigating and identifying attractive CHP and CCHP energy system design and dispatch strategies, with cold thermal energy storage for commercial buildings. Understanding multi-energy generation systems is important because of their potential to increase the efficiency of power conversion and reduce costs associated with meeting the cooling, heating and power needs of commercial buildings. We create a mixed-integer, non-linear programming model based on the CHP model developed by Pruitt et al., 2012 [47]. The model developed by Pruitt et al., contains added fidelity; off-design performance characteristics of prime movers, CO₂ taxation for natural gas and power from the macrogrid. We want to determine the design and dispatch of a CCHP system at different geographical locations and for different building types with cold thermal energy storage.

1.3 Research Objectives

Objective 1: The main objective of this study is to develop an optimization model, which determines how to design and dispatch a combined cooling, heating and power DG system with cold thermal storage. This effort includes finding the necessary level of fidelity and determining how the level of fidelity affects the calculation times and solvability of the problem.

Objective 2: The second objective of this study is to identify system designs, dispatch strategies, building types and locations most attractive for the installation of DG technologies and systems. All of the DG technologies and systems are compared against the conventional building energy systems (see Figure 3-1). In the business-as-usual case, all the power demand of the building, including meeting the cooling demand with an electric-driven vapor compression chiller, is met by the macro-grid and the heating demand by a natural gas-fired auxiliary boiler.

1.4 Thesis Overview

A literature review is presented in Chapter 2. The literature investigates different aspects of the design and dispatch of DG multi-energy generation systems with and without thermal energy storage. In addition, an overview of the different approaches available for investigating multi-energy generation DG systems is presented in Chapter 2.

Often, research efforts focus on the design problem [49] or the dispatch problem [3] of CCHP systems. By treating the design and dispatch problem separately, the global optimum is not achieved (e.g., minimizing annualized total cost). By a global optimum we mean a selection from a given domain that provides the highest value (the global maximum) or the lowest value (global minimum), minimum or maximum depends on the specific objective function. In our research effort, the given domain is the possible system designs and dispatch strategies and we are looking for the minimum total annual cost (global minimum). A significant amount of research is concentrated on both the design and dispatch of CCHP systems, but there are several gaps in the literature including the following:

- Incorporating off-design performance characteristics
- Including both hot and/or cold thermal storage
- Investigating time horizons of an entire year

Separate research efforts have concentrated on the individual characteristics listed above. However, these characteristics have not been considered simultaneously in a single, comprehensive research effort. The focus of this research is the design and dispatch problem of a CCHP system with a time horizon of an entire year. In order to realistically account for the effects of short- and long-term fluctuations of the heating, cooling and power demand, a time horizon of 365 days is necessary, to capture both daily and annual fluctuations in the cooling, heating and power demand. Optimizing over an entire year is especially important when solving the design and dispatch problem with power and/or thermal storage. With thermal energy storage, a larger fraction of waste heat can be utilized, which reduces equipment size (e.g., chillers) and improves energy management. As a simplification measure, the efficiencies of prime movers and chillers in the literature are treated as constants. Constant efficiency values are

chosen at the design point. In reality, the efficiency of prime movers and chillers is not constant and can change dramatically at part-load operation. When constant efficiencies are used, the predicted energy consumption by the prime movers and chillers is overestimated and underestimated, respectively. Thus, it is important to include off-design performance characteristics to the optimization model.

There are several approaches one can use to solve complex design and dispatch problems of CCHP systems. In the literature, the primary methods used to solve design and/or dispatch problems are [35]:

- accounting tools (RETScreen [48])
- simulation tools (HOMER Energy [25])
- optimization tools (Branch and bound, DER-CAM [37])

Studies using accounting or simulation tools do not guarantee global optimality of the solution [47] because the design and dispatch strategy must have been determined beforehand. The application of the branch-and-bound algorithm to the design and dispatch problem provides a guarantee of global optimality. Branch-and-bound methods are suitable to solve mixed-integer optimization problems. In a branch-and-bound algorithm, a systematic enumeration of all candidate solutions is performed and a large subset of fruitless candidates are discarded by using upper and lower estimation bounds of the quantity being optimized [16].

We contribute to the literature by modeling and investigating the individual elements of power-only, CHP and CCHP systems with cold thermal storage devices as well as the entire building energy system. We also identify and quantify attractive characteristics of the DG technologies, for example, the total installed cost of different SOFC systems that allow them to be economically competitive (generating savings for the building owner), as well as those of the load profiles and utility pricing structures for distributed multi-energy generation systems. The proposed optimization model accounts for off-design characteristics of prime movers and chillers, considers a whole year (365 days) as the time horizon, and allows us to analyze the effects of complex utility pricing structures and carbon taxing. Other attractive characteristics of DG technologies are the COP values of the chillers and electrical efficiency of the SOFCs.

Attractive characteristics of the load profiles are, for example, the hour-to-hour and daily fluctuation in the different energy needs of a commercial building. Other characteristics of the building and utility are the thermal-to-electric ratio of the building at a specific location and the demand charges and time-of-use electricity pricing and the difference between the price of electricity and the price of natural gas (spark spread value).

In Chapter 3, the design and performance characteristics of the individual CCHP technologies are investigated and presented. Because this research involves power-only, CHP, CCP and CCHP (multi-energy generation systems), it is also important to know how different devices are integrated with one-another (e.g., the requirements for waste heat input to the absorption chiller), the building, and the macro-grid. Also, we present analysis of the building load profiles for different building types and locations together with the analysis of the local utility pricing structures.

Chapter 4 focuses on the mathematical formulation of the large, non-convex Mixed Integer Non-Linear Program (MINLP), which is called (\mathcal{P}). The mathematical formulation considers off-design characteristics of SOFCs and the chillers, and ramping rates of the SOFCs. In this research, a linear approximation of a MINLP is solved using the branch-and-bound algorithm. The branch-and-bound algorithm requires methods to obtain global upper and lower bounds on the objective value at each node in order to converge to the optimal solution. Those upper and lower bounds can be difficult to obtain for large non-convex problems. In this study, we use problem-specific convex underestimation techniques, called (\mathcal{U}), to obtain global bounds on the objective value of (\mathcal{P}) [47]. Engineering insight into the problem motivated Pruitt et al., [47] to develop the problem-specific convex underestimation techniques. To obtain integer-feasible solutions for the global upper bounds, for (\mathcal{P}), he used linearization heuristics, called (\mathcal{H}).

In Chapter 5, we present the results obtained from the approximation of the MINLP. These results include:

- Sensitivity analysis on COP values and tax on CO₂ emissions

- Attractive characteristics building types and utility pricing structures for absorption chillers and CWS tanks

In Chapter 6, we present the conclusions from the results, as well as ideas for future work.

CHAPTER 2

LITERATURE REVIEW AND APPROACHES

2.1 Approaches and Modeling Tools

The purpose of simulation models is to mimic real life behavior [47]. A vast variety of different modeling tools and approaches have been used in the literature to solve the design and/or dispatch problem of DG systems. According to [35], there are three main categories of tools used for the investigation of DG systems. These categories are:

- Accounting tools
- Simulation tools
- Optimization tools

Accounting tools, such as RETScreen International Clean Energy Project Analysis [48], are designed for the estimation of parameters and calculation of quantities in energy efficiency and renewable energy projects. They are used to evaluate the energy production, life-cycle costs and greenhouse gas emissions of various types of renewable energy technologies and energy efficiency measures. When using accounting tools, the design and dispatch strategy of a proposed energy system needs to be pre-determined. Thus, accounting tools are not suitable for finding the optimal design and dispatch for CCHP systems with cold thermal storage.

Simulation tools are developed to describe the dynamic behavior of technologies and systems. They apply numerical techniques to perform transient analysis. A widely used simulation tool is HOMER Energy [25], developed at US National Renewable Energy Laboratory (NREL). HOMER Energy allows the user to evaluate the net present value (NPV) of both grid-tied and off-grid hybrid power systems. The disadvantage of HOMER Energy is that there is no option for thermal energy storage. In certain cases (e.g., in the presence of demand charges), sub-optimal solutions may result. Even though HOMER Energy is not the most suitable tool for finding the optimal design and dispatch of CCHP systems, it can be used as a

screening tool for comparing different technologies with one another and performing sensitivity analysis in a timely manner.

Optimization tools are developed in the literature to find the best solution (where the system design and dispatch values are variables at the beginning of the optimization procedure) in an energy system, based on selected objectives. The objective function value is either minimized (e.g., carbon emissions) or maximized (NPV). The following objective functions have frequently been applied: NPV, carbon emissions, primary energy consumption, Net Present Cost (NPC). An example of a techno-economic optimization model developed for DG adoption in buildings and micro-grids, is the Distributed Energy Resources Customer Adoption Model (DER-CAM) developed at Berkeley Lab [50]. DER-CAM is an economic model of customer-distributed, energy resource adoption; it is written as a mixed-integer linear programming model (MILP) and implemented in General Algebraic Modeling System (GAMS) language. The objective of that model is to determine the appropriate level of installed capacity and the correct dispatch strategy to minimize the global annualized cost (total energy bill) of a building or building cluster. Because DER-CAM is a MILP, it is not able to account for off-design operation of technologies such as SOFCs. In [47] Pruitt developed a MINLP model which accounts for off-design and dynamic operation characteristics of an SOFC based CHP building energy system.

The optimization model we developed in our study is based on the work of Pruitt et al., 2012 [47]. The main difference between the model developed by Pruitt and the model developed in this study is that in this study we added the cooling demand to the building energy system in addition to the heating and power demand used in Pruitt's study. Also, we separated the electric power needs for the vapor compression chiller meeting the cooling demand from the overall power demand making the overall power demand a variable (in [47] the cooling demand was incorporated into the overall building electric demand). We also added absorption chillers and CWS tanks to the building energy system model, converting the CHP system to a CCHP system with cold thermal energy system. Our research contributes to the literature by better understanding the design and dispatch of multi-energy generation systems. It considers building type, utility pricing, the presence of cold thermal storage, and building load profiles over an entire year to identify attractive characteristics of the DG technologies and of utility pricing structures and building load profiles.

2.2 Literature Review

CHP and CCHP systems are regarded as an efficient and economic means for meeting the energy needs of buildings [68]. Extensive prior work has been done on the design and/or dispatch of CHP [37] and [51] as well as on CCHP [34], [66] and [29] systems. Prior work has also been done on CCHP sub-systems, for example, coupling chillers with cold thermal energy storage devices [31] [60]. A literature review indicates that, especially in recent years, CCHP has gained a lot of interest. However, certain characteristics of CCHP systems have received less attention. Characteristics receiving less attention in the literature are: cold [31], [54] and [20] thermal energy storage, off-design and dynamic performance characteristics of chillers [21] and [68] and prime movers [34], and simulation and optimization of a system over an entire year [24] and [5]. The above-mentioned characteristics make the already difficultly distributed combined generation problem significantly harder to solve, because additional variables and parameters make the size of the problem larger and thus, harder to solve. Consequently, these characteristics are often sacrificed in order to simplify the problem. All of the characteristics of CHP, CCP and CCHP systems mentioned above have been investigated in individual studies; however, they have not been investigated together.

A combined generation system requires a prime mover that produces electric power and waste heat as a byproduct. Various different technologies have been proposed as prime movers. Most common prime movers are: Stirling engines [33], [4], micro turbines [37], [20], fuel cells [69], reciprocating internal combustion (IC) engines [37], [5], [57] and solar thermal systems [21]. In [42], current residential cogeneration systems are reviewed and compared with one another. IC engines, Stirling engines and micro turbines are all established technologies compared to fuel cell technology. Even though fuel cell technology is still relatively new, it has potential for both electricity and cogeneration applications with improved efficiency and reduced emissions. Due to the above reasons, fuel cells have been used as prime movers for power-only, CHP and CCHP energy systems in several research efforts [69] and [62].

In research efforts in which fuel cells are used as prime movers, high temperature fuel cells, such as MCFC [36] and SOFC [69], are preferred due to the availability of high grade waste heat and the ability to consume natural gas with little or no reforming. Of the high temperature fuel cells, SOFCs are the technology of choice for both residential and commercial

building applications [69], [10], [47]. Waste heat from fuel cells has conventionally been used for providing either space heating and/or hot tap water [51], [46] and [10]. One of the biggest downsides of CHP is that space-heating demand often fluctuates dramatically between seasons (Figure 3-11). Due to the reduced heating demand during summer months, the majority of waste heat needs to be vented, and, as a result, the overall CHP efficiency, as well as the economics of a prime mover, can suffer significantly. The lack of adequate heating requirements often jeopardizes the profitability of cogeneration systems [15]. Coupling a CHP plant with a thermally activated chiller device allows one to convert cooling demand into heating demand and provide relatively constant heating demand throughout the year [59], [15] and [36].

Thermally activated chillers convert a cooling demand to a heating demand. There are several options for thermally activated chillers in CCHP applications. Those are: absorption chillers, adsorption chillers and desiccant cooling. The heat source temperature limits the application of those different thermally activated chillers. The authors in [17] and [64] indicate that triple- or double- effect absorption chillers are best suited for coupling with SOFCs. Heat can be transferred from a waste heat stream into an absorption chiller through steam [66], hot water, or directly without a heat exchanger [6], [62], [61]. In [69], a direct-fired absorption chiller is coupled with an SOFC; additional heat can be added to the waste heat stream by burning natural gas. In several cases, conventional vapor compression chillers are installed together with thermally activated chillers [67], [64], [62]. Installing chillers that use different fuels, electric power, thermal energy and natural gas offers improved flexibility to respond to utility pricing and demand profile structures [5].

In [5], [27], [28] and [47] the authors make the case that it is important to look at grid-connected systems and at existing auxiliary boilers because the majority of commercial buildings are grid-connected. The presence of the macro-grid and an auxiliary boiler makes the design and dispatch of distributed combined generation significantly more flexible. The problem also becomes more complex as the number of parameters, variables and constraints is increased.

Heating and power demands seldom coincide temporally and have similar magnitudes. Hot thermal energy storage can provide desirable improved utilization of waste heat and flexibility in heating demand response [23]. In [51] and [24], the authors investigate how the addition of hot thermal energy storage to a CHP system (with an auxiliary boiler) affects the

primary energy consumption (PEC), carbon dioxide emissions (CDE), and the operational costs, as well as the design and dispatch of a CHP system. It turns out that the addition of hot thermal energy storage reduces PEC, CDE and operational costs. However, the size of the auxiliary boiler and the prime movers is not reduced significantly and buildings with low thermal-to-electric ratios do not significantly benefit from a hot thermal energy storage tank. Both of the authors utilized hourly data for an entire year to account for the fluctuation of demands between seasons. They use a trial-and-error approach for the design problem and thus, a global optimal solution is not achieved. Hot water storage tanks for hot thermal energy storage are the technology of choice due to the high thermal capacity ($\sim 4.2 \text{ kJ/kg-K}$) and low cost [19], [45], [26]. In this study we are not looking into hot thermal storage, because the buildings we are investigating have high thermal-to-electric ratios and we only look at the retrofit of the existing cooling system. The above indicates that an existing natural gas fired boiler is already in place being able to meet all of the buildings heating demand.

The benefits of cold thermal storage have been recognized in several research efforts [31], [54] and [51]. The installation of cold thermal energy storage has advantages such as: reduced chiller size, more efficient and increased flexibility of operation and load shifting capability [20]. The research in [20] indicates that, in addition to reducing the size of the chillers, chilled water storage (CWS) tanks could even reduce the installed capacity of prime movers if the cooling demand is a major contribution to the overall electric power demand. As for the type of cold thermal storage, two technologies are primarily considered: stratified chilled water storage tanks ([31], [62]) or different kinds of ice storage ([67], [60]). When water is used for thermal storage, heat is stored in the form of sensible heat. Sensible heat is energy changed between bodies due to a change in temperature of the bodies. When ice is used as thermal storage, heat is exchanged in the form of latent heat. Latent heat is heat absorbed or released at a constant temperature due to phase change. The benefit of ice storage is that ice [7] has a higher thermal capacity (less space required compared to water storage) and constant discharge temperature. CWS is a mature technology with a relatively low cost and does not require significant modifications to the existing cooling system. Any type of ice storage requires chillers which can produce liquids at subzero temperatures [7]. The drawback of chillers operating at subzero temperatures is that their COP values are lower [7], and more energy per kWh is required to remove heat from space. In [62], both hot and cold thermal storage were added to a

CCHP system meeting the energy needs of a middle-sized office in Tokyo. The design and dispatch of the CCHP system were treated as separate problems. The design problem was solved using an evolutionary algorithm, and the dispatch problem was solved separately using a linear programming algorithm. According to [47], evolutionary algorithms do not result in globally optimal solutions. In [33], compressed air is used to store energy for cooling production. However, the downside of using compressed air to run the chiller is that the size of the chiller is reduced and storing chilled water or ice promises a more significant benefit.

Commonly, a handful of representative days are used in solving the design and dispatch problem [20] of CCHP systems. The reasoning behind using 12 representative days [62] instead of all the 365 days ([51] and [24] use 365 days) of the year is reduced calculation times. Representative days do not fully capture the daily and seasonal fluctuations of the building load profiles [47]. Test runs by the author of this master's thesis, for a CCHP system with representative days, indicate that, in the presence of a CWS tank, the design and dispatch of the system is distorted. Test runs of a cooling sub-system, by the author, with 12-36 representative days indicate that a shorter time horizon benefits a larger CWS tank. A larger storage device results in a smaller cooling device and a prime mover.

In [68], the authors made the case that in order to predict the costs of a CCHP system realistically, the off-design characteristics of the equipment (prime movers and chillers) have to be included in the model. The majority of previous research neglects the off-design characteristics of prime movers and chillers to eliminate the nonlinearities from their models. Including off-design and dynamic performance characteristics of prime movers and chillers in the CCHP optimization model is important to accurately design and dispatch DG systems [47]. Results from [68] indicate that, in the presence of CWS, neglecting the off-design characteristics of chillers has only a minor effect on the overall energy consumption and cost of meeting the energy needs of a building.

2.3 Conclusions drawn from the literature review

The literature review indicates that CHP and CCHP systems can reduce the total costs, primary energy consumption and environmental impacts of meeting a building's energy needs.

The literature review shows that the installed CCHP systems are usually connected to the macro grid and have an auxiliary boiler on-site [68]. The presence of the macro-grid and the auxiliary boiler enables improved flexibility of both the design and dispatch of the entire CCHP system. Another option for improved flexibility is to install electrically driven chillers and waste heat and/or natural gas driven chillers [67]. In the study at hand, the option of installing either or both of the thermally and electric driven chillers is present. Several technologies have been used as prime movers. In this study, SOFCs are used as the prime movers because they promise higher electrical efficiencies and reduced emissions [42]. SOFCs are still in the pre-commercial stage and, thus, have a higher installed cost compared to conventional prime movers. It is expected that concerns about the environment will result in more stringent regulations [56], such that increased efficiency and reduced emissions will outweigh the increased initial cost of an SOFC. Cold thermal storage has been used for added flexibility of the design and dispatch of CHP and CCHP systems [62]. Chilled water is the most common means of cold thermal energy storage [60], [68]. The benefits of cold thermal storage include: reduced installed capacities of technologies (prime movers and chillers), improved energy (increased efficiency), economic and environmental performance of the energy system, and increased dispatch flexibility of the energy system. Most systems also use a direct-fired absorption chiller for cooling only, with the exception of [69], where the authors use the absorption chiller for providing both cooling and heating. An auxiliary boiler is used to meet the space heating and hot water needs. One paper dealt specifically with the effects of off-design operation characteristics [68].

The literature review reveals that several aspects of CCHP systems have been investigated, such as off-design and dynamic performance characteristics of prime movers and chillers, cold thermal storage, and yearly simulations and SOFCs as prime movers. However, each study neglects one or more of these characteristics because they increase the size and complexity of the design and dispatch problem. In [68], the authors investigated the most sophisticated CHP system: a design and dispatch problem for a grid-connected CHP system, with an auxiliary boiler, for an entire year. However, the authors didn't include off-design performance. A predetermined schedule for thermal storage will not ensure a global optimal solution, in [47], [29] and [30] a predetermined operating schedule is used. In [68], the authors investigated a grid-connected CCHP system with an IC engine as the prime mover, an auxiliary boiler, HWS for hot thermal storage and an absorption chiller to meet the building's cooling

demand. The off-design characteristics of the boiler, the IC engine and the chiller were included in the problem. The downside of the research effort is that the option of electric chillers was neglected and only three representative day periods are used for optimization. In [62], the design and dispatch of a grid-connected SOFC-CCHP system with an auxiliary boiler, both hot and cold thermal storage was investigated. However, this research also had several limitations. First, the design and dispatch problems are solved separately; thus, it is unlikely that a global optimal solution is achieved [47]. Second, only a two-day time horizon is used. The use of representative days is widespread in order to simplify the problem and shorten optimization and simulation times. The concern with shorter time intervals (representative days) is that the effects of seasonal demand fluctuations are not entirely grasped and the full effect of the utility pricing structure (time-of-use pricing and demand charges for power consumption) is not known. This problem is also apparent for CHP systems with hot thermal storage capacity.

Table 2-1: Summary of literature review

Paper	System	Equipment	Cooling system	Thermal Storage	Time Horizon	Off-Design	Comments
Pruitt (2012)	CHP	Aux. Boiler SOFC	N/A	HWS	365 days	SOFC	Cooling demand part of electric demand
Arcuri (2005)	CCHP	Aux. Boiler	Abs. Chiller + Compr. Heat Pump	N/A	6 days	N/A	Mixed integer model, waste heat fired heat pumps
Ehyaiei (2010)	CCHP	Boiler	Abs. Chiller + Vap. Comp. Chiller	Ice	3 days	N/A	Ice storage in hot and humid places not effective
Jiang-Jiang (2010)	CCHP	Aux. Boiler	Abs. Chiller	N/A	365 days	N/A	Cold climate benefits CCHP systems
Zhou (2013)	CCHP	Aux. Boiler IC Engine	Abs. Chiller	HWS	3 days	IC + Chiller+ Boiler	Thermal storage between IC engine and chiller and heat demand
Mago (2010)	CCHP	Aux. Boiler	Abs. Chiller	N/A	N/A	PGU + Chiller	Carbon credits benefit CCHP systems
Weber (2006)	CCHP	SOFC	Abs. Chiller + Electric Heat Pump	HWS + CWS	2 days	N/A	Design - evolutionary algorithm Dispatch – linear program
Wu (2002)	CCHP	Aux. Boiler	Abs. Chiller + Electric Heat Pump	N/A	N/A	N/A	Dimensionless energy price ratio <0.45 good for CCHP $\left(\frac{fuel}{el}\right)$
Zink (2007)	CCHP	SOFC	Abs. Chiller	N/A	1 day	N/A	Absorption chiller meets both the cooling and heating demands
Kintner-Meyer (1995)	Cooling system		Direct VCC+ Storage VCC	CWS	1 day	Chillers	Pre-cooling of building mass used as cold storage
Vetterli (2012)	Cooling system		Vapor Compression Chiller (low temp.)	Ice Storage	365 days	Chillers	50 sec. optimization run for a year using linearization techniques
Haeseldonckx (2007)	CHP	Aux. Boiler	N/A	HWS	365 days	N/A	Heat stored during one or two hours of the day
Liu (2012)	CCHP	Aux. Boiler	Abs. Chiller + Vap. Comp. Chiller	N/A	365 days	N/A	Hotel in Victoria, BC, Canada
Siddiqui (2005)	CHP	Aux. Boiler	Abs. Chiller + Vap. Comp. Chiller	N/A	365 days	N/A	Both design and dispatch of a variety of technologies

*All systems grid-connected (Except Ehyaiei et al., 2010)

CHAPTER 3

CCHP SYSTEM COMPONENTS AND INPUT DATA

In this chapter, we present and summarize the overall system configuration after which we present the performance characteristics of individual CCHP technologies. In order to predict the technical performance of the fuels cells, the chillers and the chilled water storage tanks, we need to determine the following characteristics: the variable electrical efficiency of the SOFC, the constant COP values of the chillers, the parameters of the SOFC waste heat at different stages of its utilization, and values for the temperatures and heat loss of the CWS tank. In order to account for the economic impacts of the installation of the technologies above, we need to determine the installed cost and the O&M. We also need to have the cooling, heating and power demands for both of the building types in San Francisco and Boston. The building load profiles are generated using the energy simulation software EnergyPlus, developed by the US Department of Energy. EnergyPlus has benchmark building models for both the medium sized office and the large hotel. Because the vast majority of buildings are meeting their power and cooling needs with power from the utility and their heating needs with natural gas from the utility as well, it is vital to know what the utility pricing structure are for particular locations and building types.

3.1 CCHP System

In Figure 3-1, the proposed CCHP system with cold thermal energy storage tanks is presented. Electric power and natural gas to meet the cooling, heating and power demands of a building can be purchased from the utility. We treat the building energy system as a retrofit where the cooling equipment, the vapor compression chiller and its cooling tower, is at its end of

life and needs to be replaced. Thus, we add an installed cost to the VCC. The existing natural gas fired auxiliary boiler does not need to be replaced and thus, has no installed cost tied to it. The existing equipment, or the baseline equipment, consists of an evaporative chiller and a natural gas fired boiler. There is an option to purchase additional equipment: chilled water storage (CWS) tanks, power-only or CHP-SOFCs and absorption chillers. The waste heat from the CHP-SOFC can be directed into the absorption chiller or to the absorption chiller. The costs associated with upgrading a CHP system to a CCHP system are incorporated into the installed cost of the absorption chiller [6]. Since the temperature of the waste heat leaving an absorption chiller 170°C [6] is still relatively high, the waste heat can be further utilized to meet the heating demand. A summary of cost data for the technologies considered in this study is presented in Table 3-8.

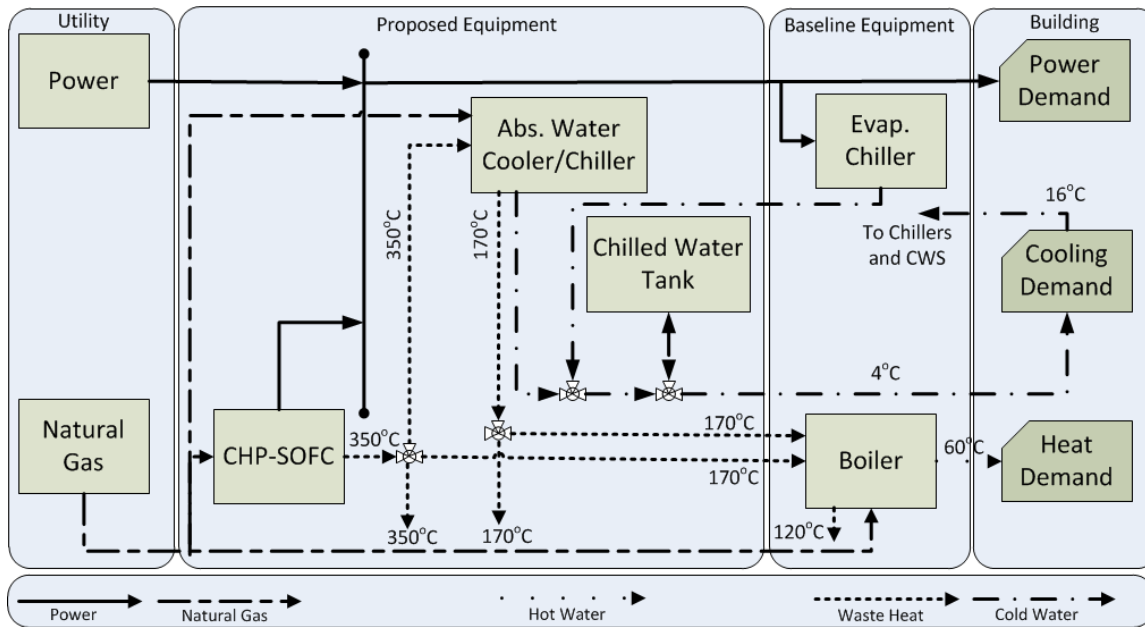


Figure 3-1: CCHP system flow diagram with CWS

In the baseline case, an existing water-cooled electric vapor compression chiller meets the space cooling demand of the building. Energy Plus analysis indicates that the original vapor compression chiller is operated in an ON-OFF mode and its COP value is around 4.5. However, in this study the COP of the vapor compression chiller is predetermined by treating the variable COP as a fixed COP, as explained in Section 3.2. At part-load operating conditions, the COP of vapor compression chillers drops, at the same time the COP of a VCC also increases with

increasing wet bulb temperatures. At higher wet bulb temperatures, the temperature difference between the condensing fluid and the cooling water decreases (making heat removal from the condenser more difficult).

The total heating demand includes the space heating and the building's hot water needs. Initially, a natural gas fired hot water boiler meets the total heating demand at a fixed efficiency. We assume that circulating hot water in radiators throughout the building provides space heating. All natural gas is purchased from the macro-grid. The power consumption of the building includes all electric power consumption except the power consumed by the existing vapor compression chiller. The electric power consumption for space cooling is subject to change, because a thermally activated absorption chiller can replace the electric driven VCC, and a CWS tank can be added to the cooling system.

In the proposed CCHP system, the acquisition of an SOFC using natural gas as fuel is considered. The CHP-SOFCs can be converted to CCHP-SOFCs with the addition of an absorption chiller. Due to their relatively high electrical efficiency, SOFCs promise lower carbon emissions compared to other DG scale, fossil-fueled, prime movers such as micro turbines, reciprocating IC engines and Stirling engines [42]. In addition, SOFCs operate at temperatures of up to $800^{\circ}C$; thus, high grade waste heat can be extracted from them, making SOFCs attractive for CHP applications [69]. By adding heat exchangers to SOFCs, high-grade waste heat can then be utilized for space heating or for the production of hot water. There are thermally activated chillers available, such as an absorption chiller, and the waste heat can be used to provide cooling. The amount of available waste heat from an SOFC is dependent on the power output and the efficiency at which the SOFC operates at that moment [47]. A fuel cell is a device that converts chemical energy from a fuel, such as natural gas, into electricity through an electrochemical reaction with oxygen (air). Usually, a fixed efficiency is used for fuel cells; however, due to the nature of fuel cells, during part load operation, the electrical efficiency of fuel cells is higher than at design point. In this study, the part load efficiencies are taken into consideration. Because fuel cells operate at high temperatures, a start-up time is necessary and fuel is used during that time to reach necessary operating temperatures, thus, a start-up cost is added like in Pruitt [47]. In addition to start-up costs, the high operating temperature prevents the

fuel cell from being turned all the way down and also limits ramping rates [47]. Both ramping rates and minimum turndown ratios are added to the SOFCs in this study.

Absorption chillers allow for the conversion of heat into cooling through the absorption process. In this study, the absorption chillers can run directly by burning natural gas (direct-fired) from the utility and/or on the waste heat from CHP-SOFCs. For simplicity, the COP of the absorption chiller is treated as a fixed value. Section 3.2 presents the reasoning behind how the COP value is achieved. In this study, the absorption chiller is only providing cooling even though absorption chillers could provide both cooling and heating [69]. Both chillers can produce chilled water and store it in a stratified chilled water storage tank. A fraction of the stored cold thermal energy is lost to the environment due to heat exchange between the chilled water in the tank and the outside.

3.1.1 Solid Oxide Fuel Cell Systems

SOFCs are devices that are capable of converting a fuel, such as natural gas, directly into electricity and heat through an electrochemical process. It is assumed that the incoming natural gas is reformed internally. During direct internal reforming, fuel is reformed into hydrogen and carbon monoxide (CO). At the same time, CO is shifted to hydrogen and carbon monoxide (CO₂). The resulting hydrogen from the reforming and shifting reacts with oxygen ions penetrating through the electrolyte. Through that reaction, electric power and heat are generated.

SOFC operating temperatures are in the 800°C range; however, its waste heat is also used to heat the air and fuel streams before entering the high-temperature SOFC in order to avoid dangerous thermal gradients in the fuel cell stack and, thus, the actual temperature of the waste heat is not around 800°C but much lower, in the 350°C. High temperature fuel cells, such as SOFCs, can use natural gas directly from the utility. A waste heat temperature of 350°C is suitable for a double-effect absorption chiller [6].

The efficiency of an SOFC is a function of its ratio of maximum output. A linear curve fit is used to represent that relationship. An R^2 value of close to 0.9 indicates a good fit. The following equation can be used to find the efficiency of an SOFC for every hour t [47]:

$$E_{jt} = \eta_j^{\max} - \left(\frac{\eta_j^{\max} - \eta_j^{\min}}{k_j^{\text{out}}} \right) \left(\frac{P_{jt}^{\text{out}}}{N_{jt}} \right) \forall t, j = 2$$

where $\eta_j^{\max} = 57\%$ is the efficiency of the SOFC at 20% ratio of maximum output, $\eta_j^{\min} = 41\%$ is the efficiency of the SOFC at 100% ratio of maximum output, k_j^{out} the size of one SOFC device, P_{jt}^{out} the electric power generated by the SOFC in hour t and N_{jt} the number of fuel cells on in hour t .

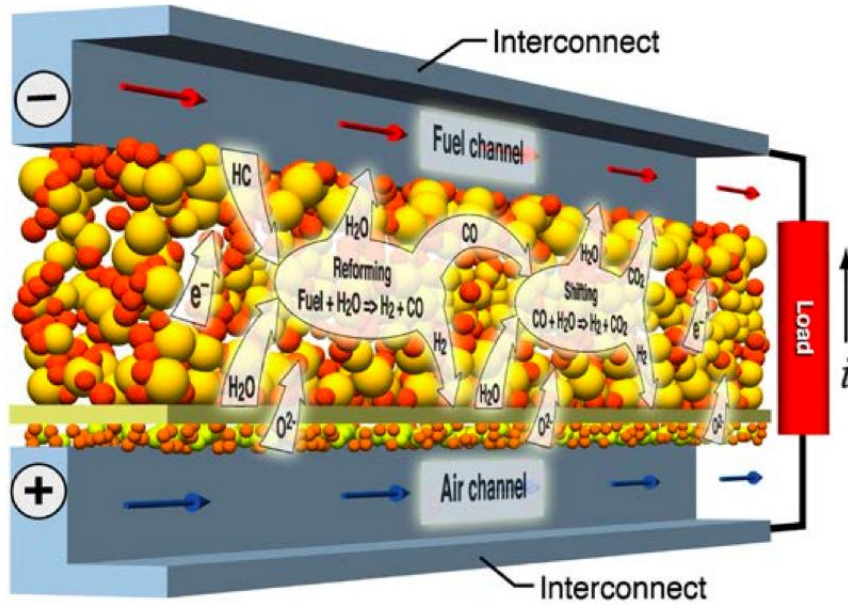


Figure 3-2: SOFC with direct internal reforming [18]

Unit installed cost of different size SOFC-CHP systems are presented in [58]. In [42], the cost and performance characteristics of different CHP systems, including different fuel cell systems, are presented. The installed cost of a power-only SOFC is taken to be \$4000/kW. According to [42], an installed cost of \$4000/kW is a reasonable assumption. In the study at hand, we are looking into SOFC systems in the 20 – 300 kW range. Authors in [58] indicate that the installed cost for such small SOFC systems in 2011 USD is \$5780/kW. The cost of heat recovery equipment has been incorporated into the installed cost of the CHP-SOFC system. According to [42], the cost of heat recovery equipment for SOFCs is an additional \$100/kW, making the installed cost of a CHP-SOFC \$4100/kW. However, preliminary results show that the installed cost of an SOFC has to be \$2000/kW for economic feasibility in Boston, making the

installed cost of a CHP-SOFC \$2050/kW. The O&M cost for a CHP-SOFC is \$0.23/kWh [42]. The O&M includes costs associated with the regular replacement of the SOFC stack. For a power-only SOFC, the O&M cost will be \$0.20/kWh, because there is less equipment in need of maintenance.

It is evident that the installed costs of SOFC systems considered in this study are rather optimistic. Installed cost includes both equipment and installation costs. However, there are several incentive programs for CHP and power-only fuel cell systems: California ([14] \$2.03 per watt of installed capacity of power-only or CHP fuel cells) and Boston (MassSave incentive program [38] offers \$750 per kW of installed capacity of fuel cell and a tax credit of \$3000/kW up to 30% of the expenditures of an installed fuel cell, from the government, through the local utility company [40]).

3.1.2 Cold Thermal Storage

Chilled water storage (CWS) tanks for cold thermal storage are an established technology. Chilled water is stored in tanks using natural stratification or other techniques to separate cold water from warm return water (Figure 3-3), and in this study we are applying the approach with the thermocline. A temperature difference of $11^{\circ}C$ is the practical maximum for many building cooling applications. Due to the temperature difference, colder water will settle towards the bottom of the tank and warm return water closer to the top of the tank. Diffusers keep the cold and warm water from mixing with one-another. A thermocline is situated between the cold and warm water mass with a large thermal gradient (we assume that it is $11^{\circ}C$), meaning that the thermocline is relatively thin compared to the cold and warm water masses [7], and the warm and cold water masses are not mixing with one another [70]. The way in which the CWS tank is stratified allows us to treat the CWS tank as a simple “kWh-counter”. A kWh-counter counts the kWh of energy entering and leaving a control surface and the difference will be the amount of “cold” energy stored or withdrawn from that control volume that the control surface surrounds (see equation 4.2c). In equation (4.9a), the energy balance of the CWS tank for each hour is calculated, and thermal losses are accounted for through the daily loss coefficient (α).

The installed cost of a CWS tank is $\$284/m^3$ [7]. That installed cost includes the tank, internal diffusers, headers and heat transfer surface. Thermal conduction losses to the environment occur with a rate of 1 to 5% of storage capacity per day (a value of 3% is used in this study). The main benefits of CWS tanks are that the existing chillers can be used and the CWS tank can also perform fire protection duty. It is assumed that the O&M costs of the CWS tank are negligible.

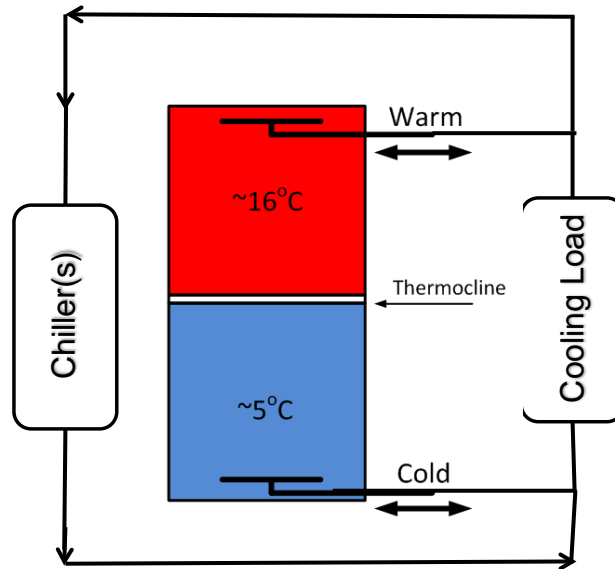


Figure 3-3: Stratified CWS tank [7]

By treating the temperature of the cold and warm water masses as constants, a question arises: what will happen if the water tank is empty (water temperature will rise when the tank is empty due to heat gains from the environment)? The results from the cases investigated in this study show that the level of cold water mass will only drop to 0 at the end of the time horizon, indicating that the CWS tank is used daily.

3.1.3 Vapor Compression Chillers

Vapor compression chillers are devices that can remove heat from a colder environment, a building, and transfer it to a warmer environment, the outdoors, by shifting the boiling/condensing temperature of a refrigerant fluid through altering its pressure. In order to increase the pressure of vapor it needs to be compressed. Compressing vapor requires work

input, conventionally in the form of electric power. The installed cost of a VCC system consists of the cost of the chiller itself and the cost of the heat rejection equipment (cooling towers).

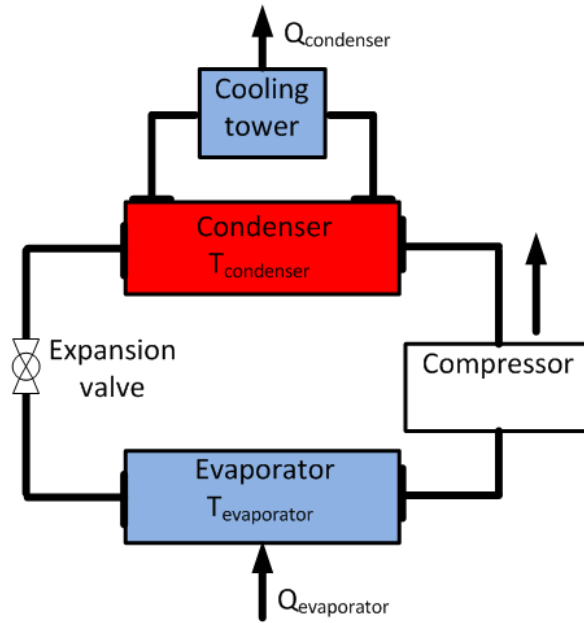


Figure 3-4: Vapor compression chiller

The cost of heat rejection equipment is obtained from [6] by dividing the required heat rejection equipment for an absorption chiller by 2, as a VCC transfers approximately half of the heat compared to an absorption chiller. Operation and maintenance costs have been incorporated into the capital costs of a VCC and are approximately 4% [33] annually of the installed costs. The total installed cost of a VCC system including the heat rejection equipment is \$365/kW (\$105/ton). Installed costs are usually higher than capital cost because labor and engineering costs have to be added, and for that reason the capital costs of the VCC has been multiplied by a factor of 1.8 [39]. The COP of the VCC is presented in Section 3.2.3.

3.1.4 Absorption Chillers

The main difference between absorption chillers and VCCs is that in an absorption chiller liquid is being compressed instead of vapor. Compressing vapor is significantly more efficient. Liquid can be compressed instead of vapor because an absorption process is used to convert vapor into liquid before it's compressed. Additional external heat is required to keep that

absorption process running. Natural gas and/or waste heat can be used as the external heat source and, in this study, both can be used as external heat sources. In general, waste heat and natural gas are cheaper than electricity from the grid. However, absorption chillers are significantly more expensive compared to VCCs. Due to the high installed cost of absorption chillers, VCCs are often preferred over absorption chillers.

We are using an SOFC as a prime mover. From [64], the authors indicate that the properties of the waste heat of an SOFC match with the input parameters of a double-effect absorption chiller. Double-effect absorption chillers have the benefit of a higher COP of 1.2 compared to around 0.6 for single-effect absorption chillers.

In Figure 3-5, we present the flow diagram of a double-effect absorption chiller. The Yazaki absorption chiller-heater uses a solution of lithium bromide and water, under a vacuum, as a working fluid. Water is the refrigerant and lithium bromide is the absorbent. The double-effect absorption cycle has two generators – one directly heated by a gas burner and the other heated by hot refrigerant vapor. Refrigerant, liberated by heat from the solution, produces a refrigerant effect in the evaporator when cooling water is circulated through the condenser and absorber [65]. In cooling mode, heat is being removed from the absorber and condenser by cooling water and rejected to the environment in a cooling tower.

The total equipment cost is obtained from ASHRAE handbooks [6]. The capital cost includes the chiller itself and the heat rejection equipment (water cooling tower). The equipment costs are multiplied by a factor of 1.8 to get installed costs. The equipment cost is converted from 1994 USD to 2011 USD using the Chemical Engineering Plant Cost Index (CEPCI) averaged over a year. Similarly to the VCC, the O&M of the absorption chiller equipment is a fixed annual fee of 4% of the total installed cost of the absorption chiller. The O&M is added to the amortized annual cost. The total installed cost of a double-effect absorption chiller used in this study is \$754/kW (\$214/ton).

In [69], a direct-fired absorption chiller is used, and the absorption chiller can directly utilize waste heat. In [6], the waste heat exiting the absorption chiller has to be above $170^{\circ}C$, in order to avoid condensation. Thus, the gradual waste heat from the absorption chiller can be sent

to heat up water to meet the heating demand of the building. It is assumed that the waste heat exiting the heat exchanger for heating purposes is $120^{\circ}C$.

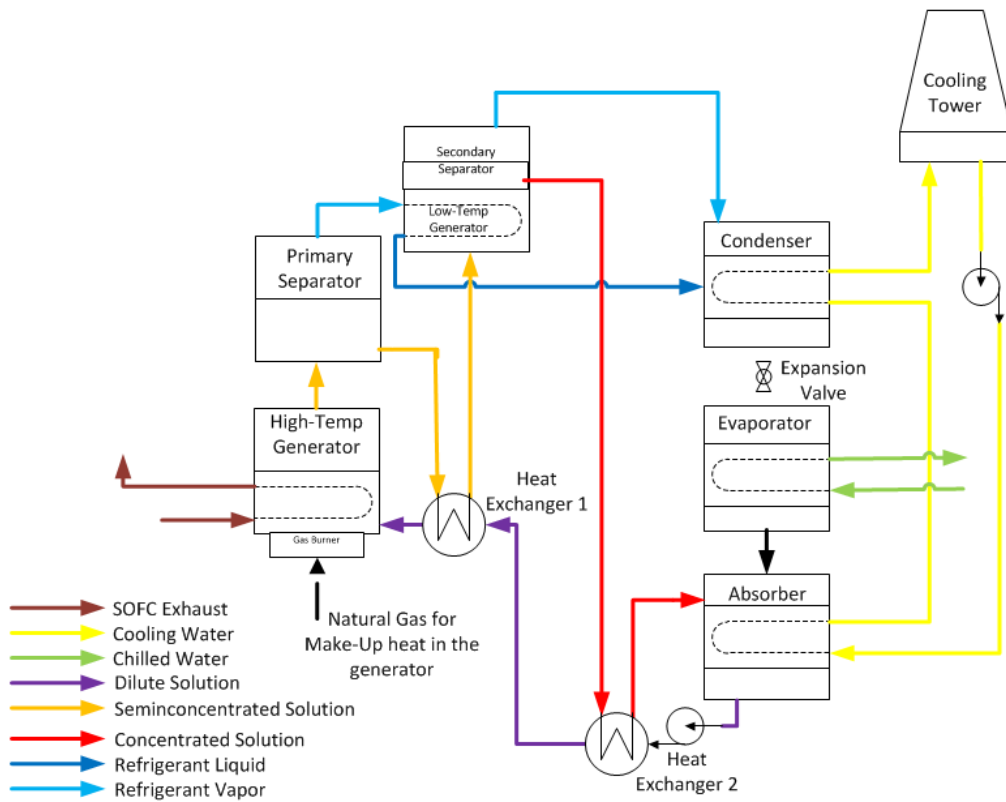


Figure 3-5: Double-effect absorption chiller [65]

3.2 Chiller COP values

In many research efforts [69], the COP of both absorption and vapor compression chillers is treated as a constant value. However, the COP of a chiller is a function of the part load ratio of the chiller and the wet bulb temperature. The wet-bulb temperature is the temperature a parcel of air would have if it were cooled to saturation (100% relative humidity) by the evaporation of water into it, with the latent heat being supplied by the parcel [63].

3.2.1 Absorption Chiller COP

In Figure 3-6, we present the part load capacity chart for a double effect lithium bromide (LiBr) absorption chiller. The fraction of design heat input is dependent both on the part load ratio (f_{PLR}) as well as the temperature of the cooling water. In this study, we use the COP of a chiller; thus, we converted the above relationship (Figure 3-6) between part load ratio and the design heat input into a relationship between the part load ratio and the COP (Figure 3-7). In addition, the entering cooling water temperature has been converted into the outdoor wet bulb temperature, as we are utilizing the wet bulb temperature for different locations gained from EnergyPlus simulation runs. In Figure 3-11, the part load ratio is the x in the curve fits and y is the COP value. We perform curve fitting of the COP functions in Figure 3-7 to obtain equations for the COP as a function of the part load ratio and the wet bulb temperature.

Curve fitting results in R^2 values of above 0.95 indicating that a second order polynomial is an accurate fit. The temperature of the cooling water is a function of the wet bulb temperature [6], [8]. The difference between the wet bulb and cooling water temperature for an indirect water-cooling tower at design point is 4°C [8]. We assume that the pinch (difference between wet bulb temperature and cooling water temperature) is constant for all wet bulb temperatures. In order to assess the COP in every hour, an equation for calculating COP is generated from the curve fits, and the polynomial function constants are averaged values from Figure 3-7:

$$COP_{6t} = -0.857 \left(\frac{Q_{6t}^{out}}{k_6^{out} N_{6t}} \right)^2 + 1.135 \left(\frac{Q_{6t}^{out}}{k_6^{out} N_{6t}} \right) + [1.854 - 0.025(\Delta\tau_t^{wb})]$$

where $\Delta\tau_t^{wb}$ indicates the wet bulb temperature above $-21^\circ C$ in hour t .

The wet bulb temperature difference ($\Delta\tau_t^{wb}$) is used to account for changes in the COP value due to changes in the wet bulb temperature. The value of 0.025 indicates the extent to which the COP curve shifts downwards with a temperature increase of $1^\circ C$. The numerical value 0.25 is obtained as follows:

$$\frac{a_0^{\tau_{min}^{wb}} - a_0^{\tau_{max}^{wb}}}{\tau_{max}^{wb} - \tau_{min}^{wb}}$$

where, a_0 is the coefficient in a_0x^0 from the polynomial curve fit in Figure 3-7, τ_{\max}^{wb} is the maximum wet bulb temperature (25°C in this case) and τ_{\min}^{wb} is the minimum wet bulb temperature (9°C in this case). It is assumed that the value 0.25 is constant over the entire wet bulb temperature range, where the wet bulb temperature -21°C is the lowest wet bulb temperature in Boston.

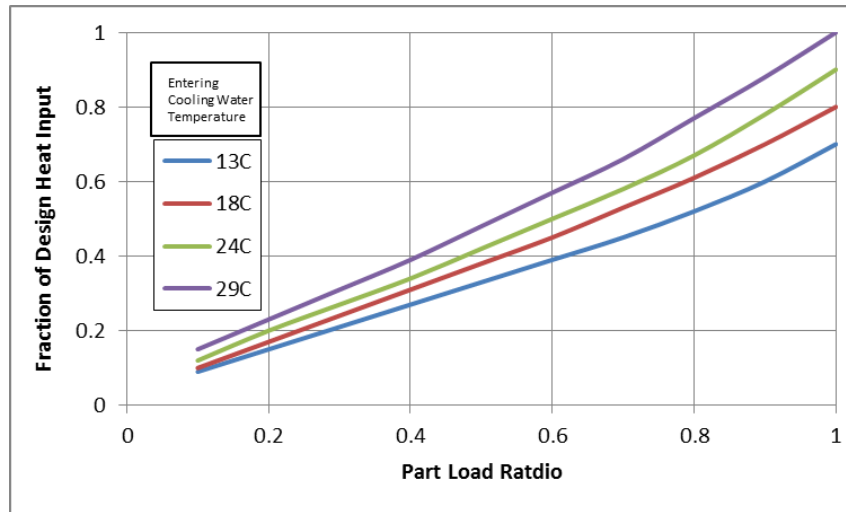


Figure 3-6: Part load operation, double-effect absorption chiller [6]

3.2.2 Vapor Compression Chiller (VCC) COP

In Figure 3-9, we present the part load capacity chart for a vapor compression chiller. The COP of the chiller is a function of the part load ratio that the chiller is operating at in a given moment and the wet bulb temperature. In Figure 3-9, the part load ratio is the x in the curve fits and y is the COP value. Again, the entering cooling water temperature has been converted into the outdoor wet bulb temperature.

We perform curve fitting of the COP functions in Figure 3-9. Curve fitting results in R^2 values of close to 1, indicating that a second order polynomial is an accurate fit. The temperature of the cooling water is assumed to be a function of the wet bulb temperature (Figure 3-8) with a pinch of 4°C [8]. In order to assess the COP in every hour, we generate an equation for calculating COP from the curve fits like we did for the COP of the absorption chiller:

$$COP_{5t} = -4.91 \left(\frac{Q_{5t}^{out}}{k_5^{out} N_{5t}} \right)^2 + 8.32 \left(\frac{Q_{5t}^{out}}{k_5^{out} N_{5t}} \right) + [2.22 - 0.021(\Delta\tau_t^{wb})]$$

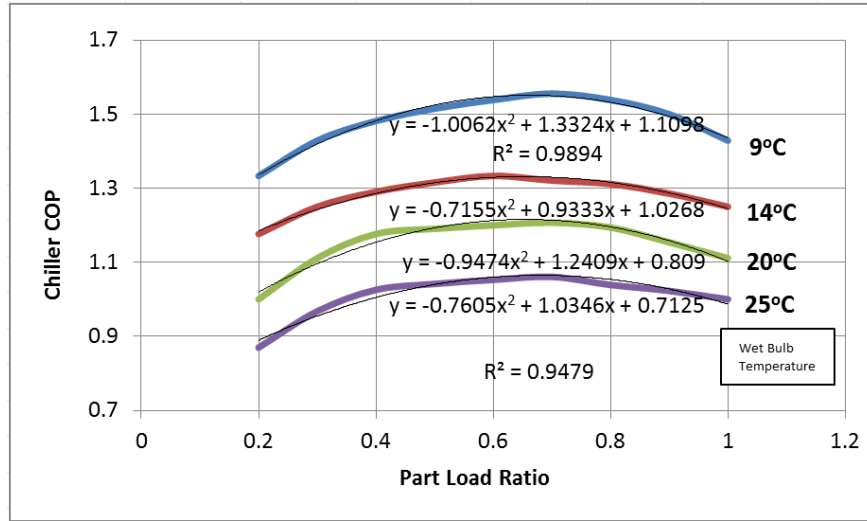


Figure 3-7: COP, double-effect absorption chiller

3.2.3 COP analysis (VCC and absorption chiller)

In the table below, we perform the COP value analysis for both of the chillers. The COP of both of the chillers depends on the part load ratio (f_{PLR}) and the wet bulb temperature ($\Delta\tau_t^{wb}$). The results in Table 3-1 are created by using the cooling load profiles of the building types and the locations listed. The annual cooling load peak is determined, and then the above equations are used to find the COP values for both of the chillers for every hour of the year. The hours at which the building had no cooling load are not included in the average COP value calculations. When larger chillers are being installed, the parameter (k_5^{out}) obtains a larger value and thus, the chillers will operate more frequently in part load mode, lowering the average COP. There are two extreme cases; in the first case, the chiller is as big as the maximum cooling load, e.g., 800 kW for a large hotel in Boston (resulting in the COP_{min}), in the second case, many individual chillers with a relatively small size will be installed, e.g., 800 1 kW chillers (resulting in the COP_{max}).

In the first case (one large chiller), the chiller operates most of the time at part load and in the second case (many small chillers), the chillers operate most of the time at their design load.

However, it is unlikely that 800 chillers with a size of 1kW will be installed in a large hotel in Boston (see Table 3-5). In Table 3-5, the difference in energy consumption is presented between the cases when 1 chiller is installed compared to many 1 kW chillers. The energy consumption of an absorption chiller doesn't change by much compared to a VCC and for that reason is not adjusted between a CWS and a no CWS optimization run.

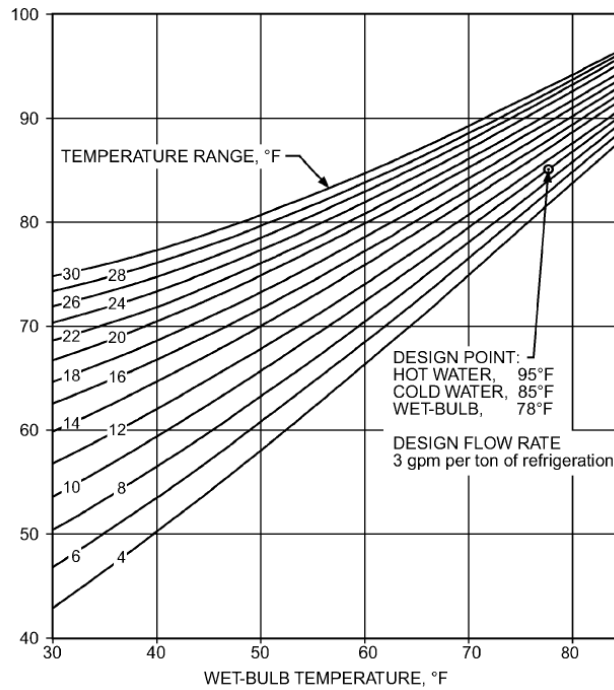


Figure 3-8: Cooling tower performance – 100% design flow [8]

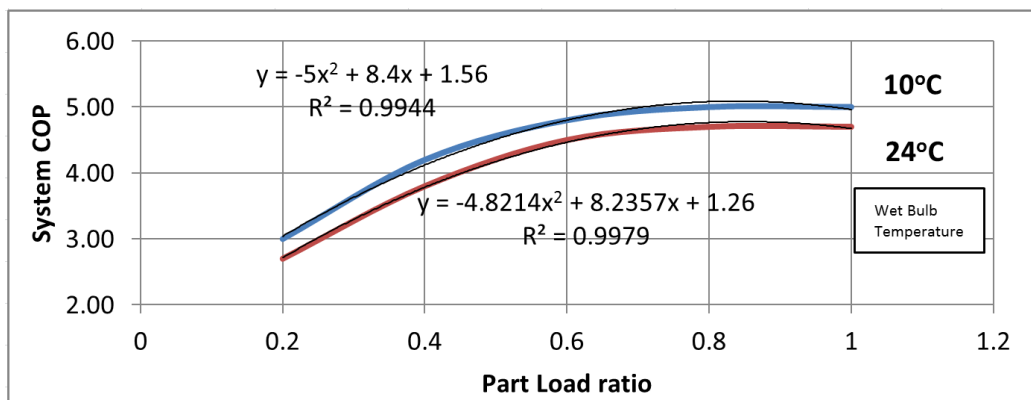


Figure 3-9: COP of VCC [66]

In this study, the largest chiller size requirement is for a large hotel in Boston where the peak cooling demand is around 800 kW (227 ton). Consulting an industry contact [1], we learned

that cooling capacities in the range of 800 kW require only one chiller (installing more than one unit would increase the costs significantly).

Table 3-1: COP_{min} and COP_{max} of chillers

Building Type		Large Hotel			Medium Office		
Location		Los Angeles	Boston	San Francisco	Los Angeles	Boston	San Francisco
ABS Chiller	COP _{min}	1.239	1.270	1.268	1.209	1.200	1.224
	COP _{max}	1.327	1.406	1.329	1.239	1.211	1.287
	Change in Energy Consumption	-2.5%	-0.2%	-0.9%	-2.24%	-4.93%	-1.16%
VCC	COP _{min}	3.575	2.745	3.259	3.482	3.703	3.241
	COP _{max}	4.898	5.020	4.956	4.879	4.857	4.921
	Change in Energy Consumption	-20.5%	-28.9%	-28.8%	-21.3%	-19.4%	-23.5%

Taking the above into consideration, it is not justified to use the “COP_{max}” value as the fixed COP for chillers, especially for VCCs, a value closer to the “COP_{min}” should be used. The “COP_{min}” cannot be used directly.

Table 3-2: Adjusted COP values for VCC

Building Type		Large Hotel			Medium Office		
Location		Los Angeles	Boston	San Francisco	Los Angeles	Boston	San Francisco
VC Chiller	COP _{min}	3.932	3.396	3.562	3.914	3.814	3.825
	COP _{max}	5.143	4.794	5.183	6.075	4.736	6.594

When using the “COP_{min}” value as the COP for chillers the cost of electric power consumed will be overestimated. During high demand, the average COP (“COP_{min}”) is lower than the actual COP. During nighttime operation, at low ambient temperatures, the average COP (“COP_{min}”) value will again be lower than the actual COP.

Table 3-3: COP of VCC with and without CWS

	Building Type	Large Hotel		Medium Office	
	Location	Boston	San Francisco	Boston	San Francisco
VC Chiller	COP _{min} (No storage)	3.396	3.562	3.814	3.825
	COP (Storage)	3.532	4.394	4.229	6.058
	COP _{max}	4.794	5.183	4.736	6.594

Thus, we need to adjust the “COP_{min}” values when a CWS tank is installed to reflect the improved COP resulting from higher capacity factors. The location and building type-specific adjusted “COP_{min}” value is used when no CWS is present, because the output of the chiller will fluctuate significantly. However, when CWS is present, we expect that the chiller will operate closer to its design point. In Table 3-3, we present the comparison of the capacity factor of the chillers with and without cold thermal storage. Based on Table 3-2 it is not justified to use “COP_{max}” for the cases with CWS; instead, we assume that there is a linear relationship between the COP and the CF and linear interpolation is used to find the appropriate COP values for cases with CWS.

3.3 Building Types and Locations

LeMar [32] investigated both the potential of CHP and CCHP by building type and location. The authors concluded that office buildings present the biggest market for both CHP (potential of ~5800 MW of total installed capacity) and CCHP (potential of ~4000 MW) installations due to the sheer number of office buildings in the US. Hotels present a significantly smaller potential for the overall installed capacity for CHP (potential of ~1000 MW) and CCHP (potential of ~500 MW) applications. The large and coincident power, heating and cooling loads (Figure 3-10 and Figure 3-13) make hotels attractive for CHP and CCHP installations.

Figure 3-10 and Figure 3-13 show that the cooling, heating and power load profiles of a large hotel have a significantly higher baseload compared to a medium sized office building. A high power demand baseload means that a relatively large prime mover, such as an SOFC, can operate at close to its design power most of the time of the year. In addition, the cooling, heating and power load profiles have relatively similar patterns, meaning that a large portion of the available waste heat can be utilized for either cooling or heating together with electric power. Homer Energy [25] evaluates the day-to-day and time-step-to-time-step random variability of the power, heating and cooling demand profiles, standard deviation in the sequence of daily averages and the standard deviation in the difference between the hourly data and the average daily profile, respectively. In Those random variability terms are used by Homer Energy to describe load profiles of buildings [25].

Table 3-4, the random variability values for the power demand of a medium office and a large hotel in San Francisco are presented. The values indicate that the power demand of a large hotel stays relatively constant between hours and the daily averages are very similar as well. Those random variability terms are used by Homer Energy to describe load profiles of buildings [25].

Table 3-4: Random variability of power demand in San Francisco, CA

Random Variability	Medium Office	Large Hotel
Day-to-day	38.8%	2.05%
Time-step-to-time-step	45%	5.75%

Table 3-5: Thermal-to-electric ratios

	Medium Office	Large Hotel
San Francisco	0.181	0.699
Boston	0.506	0.181

A “smoother” load profile allows one to maintain high capacity factors (CF) of relatively large prime movers, compared to the annual peak demand. The prime mover can operate in a load following mode.

The capacity factor of a prime mover has a direct impact on the cost of electricity generated by that prime mover [11]. In addition to analyzing building types, the authors in [32] performed a regional analysis of market potential for CHP and CCHP systems. The multi-generation energy systems at hand are using natural gas as fuel (because of the existing natural gas distribution infrastructure). Location specific spark spread values are obtained by subtracting the cost of natural gas ($\$/kWh$) from the cost of electricity ($\$/kWh$). Locations with high spark spread values promise the highest market potential to distributed multi-energy generation systems because power can be generated on-site from natural gas at lower cost compared to the power from the macro-grid. According to the LeMar [32], the New England region and California pose the most favorable market potential for distributed CHP and CCHP applications. Considering the above regions, Boston and San Francisco are the two cities investigated in this study.

3.3.1 San Francisco

San Francisco is chosen as a location due to the high cost of electricity with a complex pricing structure (time-of-use pricing structure for energy charges and demand charges) and relatively low natural gas prices. In addition, carbon emissions from the macro-grid in California are among the lowest in the US, allowing one to compare how a tax on low and high CO_2 emission rates affects the design and dispatch decision. The reason behind time-of-use energy charges and demand charges is that it is expensive for the utility companies to meet peak energy demand

3.3.1.1 Load profiles

Investigation of the load profiles of San Francisco (see Figure 3-10), for the large hotel, indicates that the cooling, heating and power demands are close to concurrent. The availability of

sufficient heating and cooling loads in a large hotel means that a large portion of the available waste heat from the prime mover can be utilized. However, the load profiles of a medium office demonstrate (see Figure 3-10) that the heating demand is significantly smaller compared with the power demand; and, a CHP system can result in venting some of the waste heat. A CCHP allows one to utilize a higher fraction of the available waste heat from a prime mover by converting cooling demand into heating demand, resulting in a stable heating demand all year round.

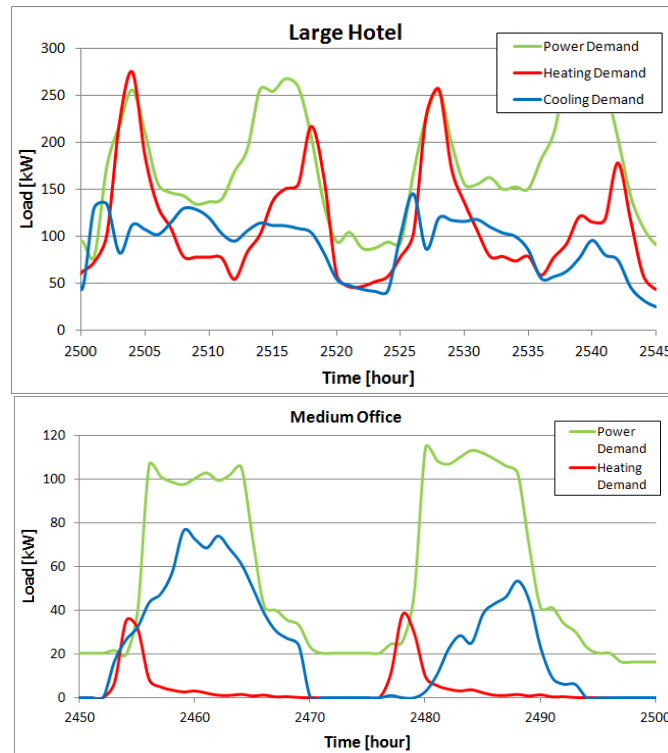


Figure 3-10: Building Energy Load profiles in San Francisco, CA

Figure 3-11 shows that heating demand in a medium office might not be sufficient to utilize all the waste heat from an SOFC. The thermal-to-electric ratio of a medium sized office in San Francisco is especially low, compared to the large hotel and the medium sized office in Boston (see Table 3-5), indicating that a significant portion of waste heat could be vented in a medium sized office in San Francisco. The load profiles of a large hotel are fluctuating significantly less between seasons and days (see Figure 3-10 and Figure 3-11) promising that a prime mover can meet a larger fraction of the power demand without sacrificing its capacity factor.

3.3.1.2 Utility

The utility pricing structure for a commercial customer in San Francisco is presented in Table 3-6. It can be seen that natural gas is significantly cheaper than electricity. In addition, there is a significant difference between off-peak and peak energy charges. The difference between peak and off-peak energy charges creates motivation for load shifting, and the presence of demand charges is a motivation for implementing peak shaving. Peak demand charges are applied by the utilities to cover their costs associated with meeting the peak electricity demands with peaking power plants. The cost of electricity from a peaking plant is more expensive because they have low utilization (low capacity factors) and usually run on more expensive fuels (natural gas) compared to baseload power plants (coal or nuclear).

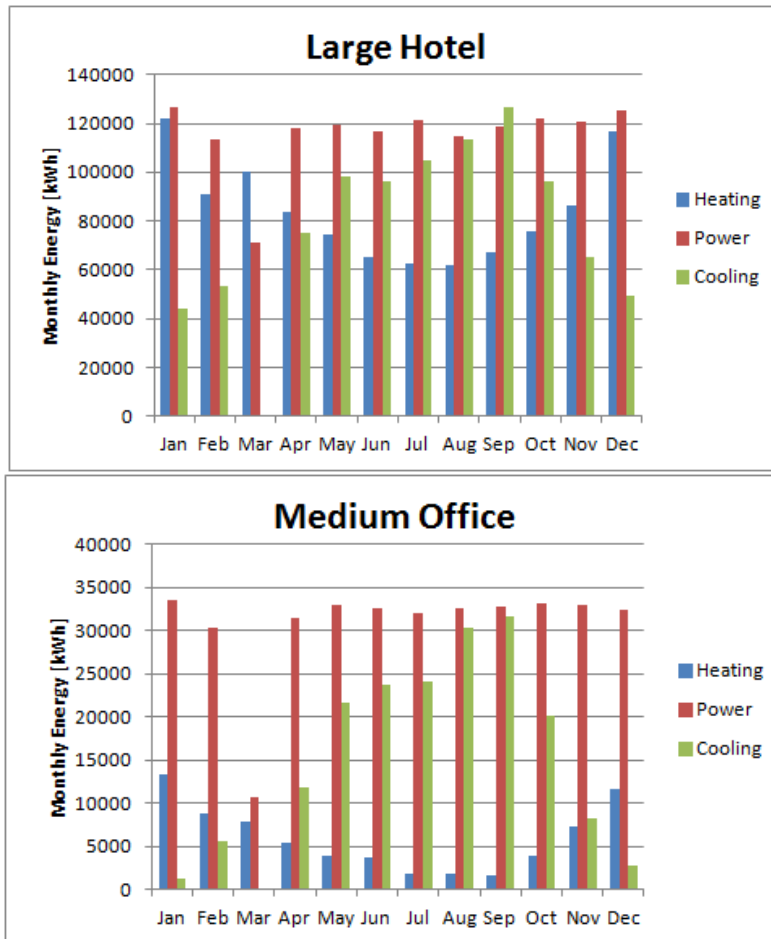


Figure 3-11: Monthly energy consumption in San Francisco, CA

Braun et al., 2010 [11] shows that a low capacity factor and high fuel costs increase the cost of electricity from a power plant. Electricity pricing data is acquired from Pacific Gas and Electricity [43], and the A-10 time-of-use schedule is used. Natural gas prices are obtained from Pacific Gas and Electricity [43], the G-NR1/2 schedule (general non-residential) is appropriate for the large hotel and medium sized office building. According to the Environmental Protection Agency [22], carbon emissions from the California grid are 0.256 kg/kWh.

3.3.2 Boston

Boston is chosen to be one of the locations to investigate CCHP systems in our study because of the very high demand charges (\$/kW) applied for monthly peaks and low energy charges (\$/kWh), the relatively high carbon emissions for power consumption from the grid, and different climate compared to San Francisco.

3.3.2.1 Load profiles

Similar to the load profiles in San Francisco, the different loads of a large hotel (cooling, heating and power) follow similar patterns by having two peaks (see Figure 3-13). There is also a significantly larger heating demand for a medium office in Boston, compared to San Francisco, thus we assume that a medium office in Boston benefits less from upgrading a CHP system to a CCHP system.

3.3.2.2 Utility

The utility pricing structure of Boston differs significantly from San Francisco (compare Table 3-6 with Table 3-7). The main difference is that the demand charges in Boston are significantly higher than in San Francisco, and the energy charges are much lower in Boston compared to San Francisco.

In addition, time-of-use pricing is used in San Francisco, while a flat rate is used in Boston. The difference in utility pricing structures between these two locations allows us to

evaluate the effects of time-of-use pricing versus demand charges. According to the Environmental Protection Agency [22], CO_2 emissions from the Massachusetts grid is 0.56 kg/kWh.

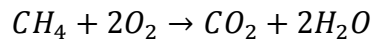
Table 3-6: Utility rates in San Francisco A-10, CA [52][53]

	Summer	Winter
Off-Peak	9¢/kWh	8¢/kWh
Mid-Peak	14¢/kWh	9¢/kWh
Peak	21¢/kWh	-
Peak Demand Charge	\$6.39/kW	\$6.39/kW
Natural Gas	2¢/kWh	2¢/kWh

*This rate has peak and off-peak periods. Peak is from 12 p.m. to 6 p.m. weekdays from June through September. Mid-peak is from 8 a.m. to 12 p.m. and from 6 p.m. to 11 p.m. weekdays from June through September and 8 a.m. to 9 p.m. weekdays October through May. Off-peak is all other hours including weekends and the California holidays.

3.3.3 CO_2 emission rate from natural gas

We assume that natural gas at both locations consists mainly of methane (CH_4). The (CO_2) emission rate ($\$/kWh$) from natural consumption by the SOFC and the boiler is obtained from the molar balance of completely combusting methane (CH_4):



The above equation indicates that the combustion of one mole of natural gas results in one mole of CO_2 emissions. The molar mass of CH_4 is 16 g/mol, and the molar mass of CO_2 is 44 g/mol. From [25], the energy content of natural gas is 12.5 kWh/kg (LHV). Unit conversion results in a CO_2 emission rate of 0.22 kg $_{CO_2}$ /kWh.

Table 3-7: Utility rates in Boston, MA [40]

	Summer	Winter
Distribution Energy	0.88¢/kWh	0.88¢/kWh
Distribution Demand	\$11.43/kW	\$19.88/kW
Transition Energy Peak	0.465¢/kWh	0.465¢/kWh
Transition Energy Off-Peak	0.465¢/kWh	0.465¢/kWh
Transition Demand	\$1.66/kW	\$1.66/kW
Transmission Demand	\$7.08/kW	\$7.08/kW
Energy Conservation	0.25¢/kWh	0.25¢/kWh
Renewable Energy	0.05¢/kWh	0.05¢/kWh
Natural Gas	3¢/kWh	3¢/kWh

*This rate has no peak and off-peak periods. Summer demand charges apply from June through September; and winter rates apply from October through May.

3.4 Summary of Input Data

In Table 3-8 below we present the summary of the cost parameters of the proposed technologies as well as the key operating parameters.

3.5 Assumptions

Because the model presented in this thesis is only a representation of a real life system, several simplifying assumptions have been made:

- Waste heat utilization: Waste heat from the SOFC can be utilized for heating and/or cooling or be vented. In case waste heat is used for heating, the temperature of the exhaust drops from 350°C (assumed to be constant) down to 120°C. However, when waste heat is used in the absorption chiller, the temperature of waste heat drops from 350°C down to

170°C, to avoid condensation. Waste heat from the absorption chiller can be vented or utilized further for heating by dropping the temperature of waste heat from 170°C down to 120°C.

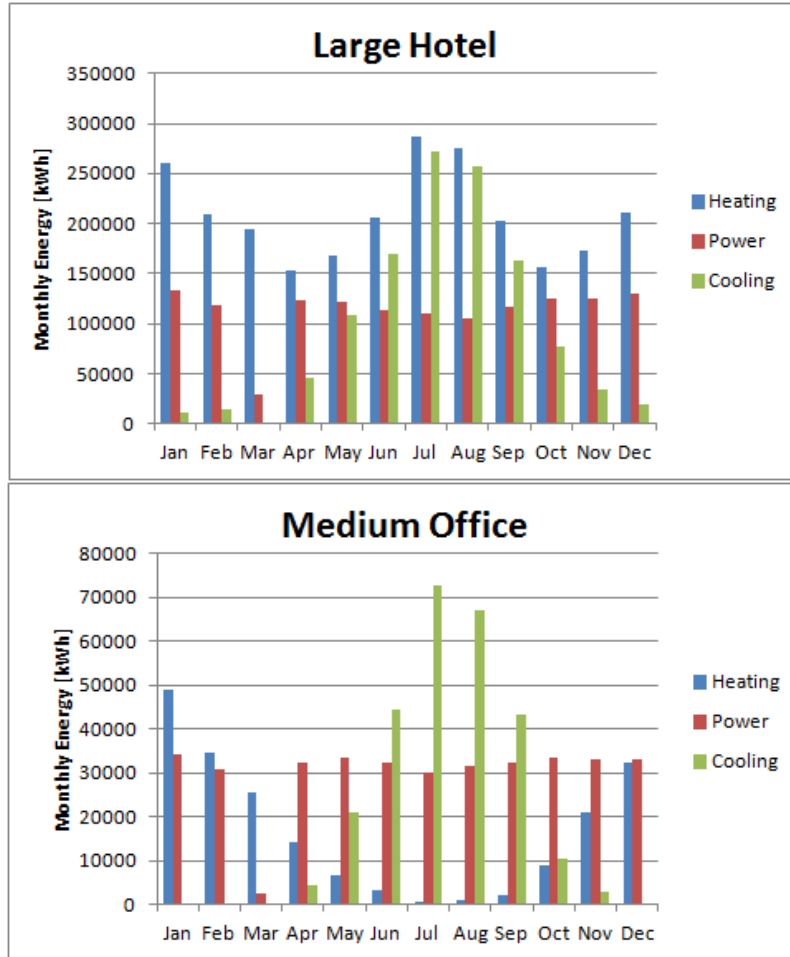


Figure 3-12: Monthly energy consumption in Boston, MA

- The electrical efficiency of an SOFC is only a function of the part load ratio.
- The efficiency of the auxiliary boiler is a constant of 80%.
- It is assumed that the warm and cold water masses do not mix with one another and a constant temperature can be maintained on each side of the thermocline. In addition, it is assumed that both the charging and discharging temperatures of the CWS tank are equal to the temperature of the cold-water mass below the thermocline. Heat gains from the environment in every hour are considered to be a constant.

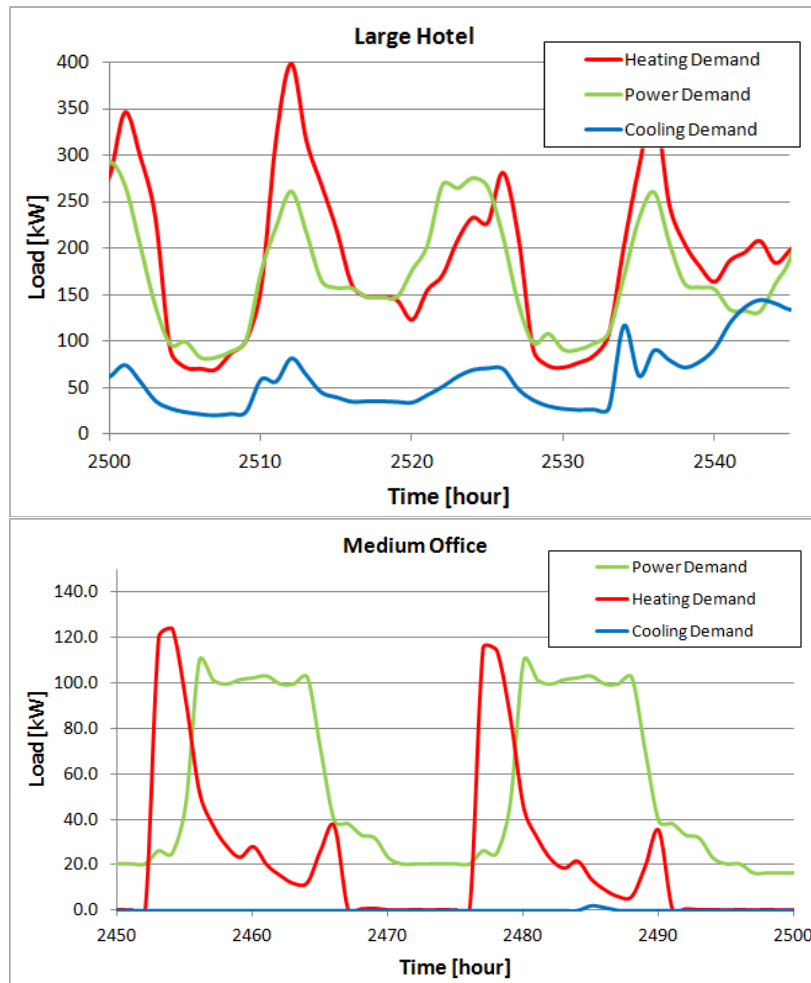


Figure 3-13: Building energy load profiles in Boston

Table 3-8: Summary of technology input parameters

Device	Installed Cost	O&M	Efficiency/ COP	Turn down ratio
SOFC	\$4000/kW	¢2/kWh [42]	41-61% _e [47]	0.2 [47]
CHP-SOFC	\$4100/kW	¢2.3/kWh [42]	41-61% _e [47]	0.2 [47]
Water Cooled Double-Effect Absorption Chiller	\$625/kW (\$2200/ton) [20]	\$30/kW-year [32]	~1.2 [6]	0
Water Cooled Vapor Compression Chiller	\$370/kW (\$1300/ton) [7]	\$15/kW-year [32]	~3.4-6.1 [66]	0
Chilled Water Storage Tank	\$280/m ³ [7]	N/A	N/A	0

- Even though the COP of a chiller varies with the wet bulb temperature and the part load ratio, it is considered to be a constant in this study. Based on information gained from industry contact [1] it is assumed that only one chiller from each chiller type is installed to meet the cooling demands of a building.

CHAPTER 4

MODEL

In this chapter, we present the optimization model, (\mathcal{P}), to determine the optimal design and dispatch of a CCHP system. The objective function of this optimization model is to meet the cooling, heating and power demand of a commercial building for an entire year at the lowest total annual cost. The model determines the design and dispatch of the existing equipment, the proposed equipment (chillers, thermal storage and SOFC systems), and the exchange of power and natural gas from and to the utility. In order to give a better understanding of the existing and proposed equipment and the ways the different technologies interact with one another, we presented an overview of the proposed system configuration and all the individual technologies in Section 3.1. In Section 3.1 we also described the parameters, variables, objective, and constraints in the system model. At the end of this chapter, we present a detailed mathematical formulation for the CCHP optimization model called (\mathcal{P}). The optimization model is based on the work of Pruitt et al. [47].

4.1 Distributed CCHP Generation System

The distributed CCHP generation system under consideration is presented in Figure 3-1. The system consists of the utility (electric power and natural gas), the proposed, as well as the existing, equipment and the energy requirements of the building. Three energy needs of the building are considered. Those energy needs are: space cooling, heating (both hot tap water and space heating), and the general electric power demand. Both natural gas and electricity can be purchased from the grid.

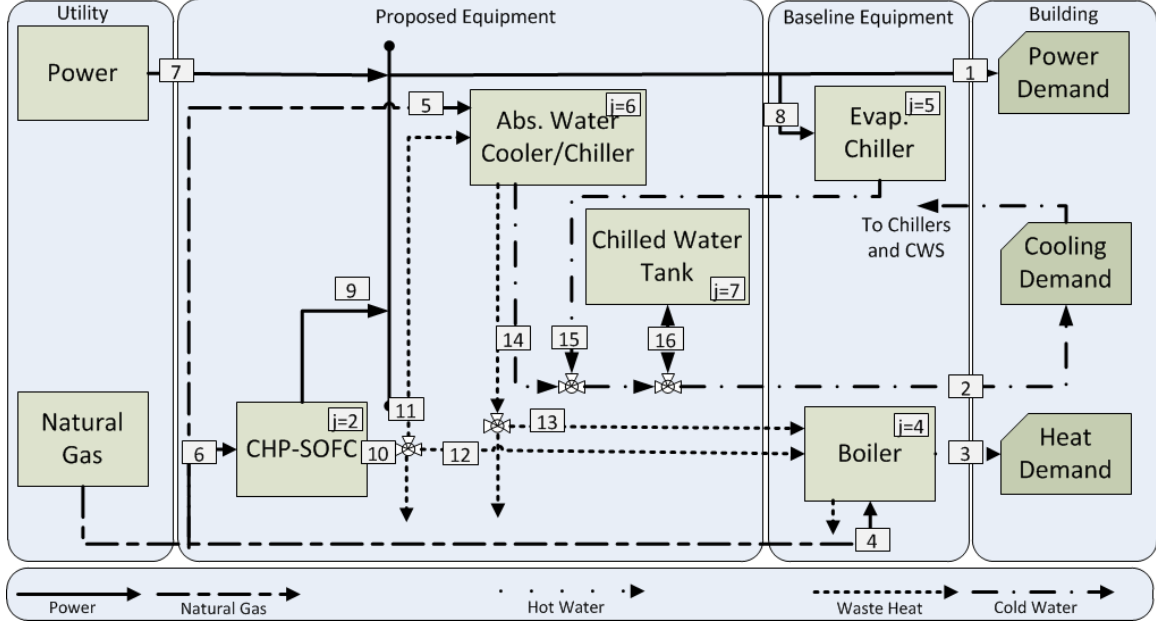


Figure 4-1: CCHP system diagram

* 1) Non-AC power electric power demand of the building (d_t^P) [kW] in hour t , 2) cooling demand of the building (d_t^C) [kW] in hour t , 3) total heating demand of the building (d_t^Q) [kW] in hour t , 4) natural gas consumed by the auxiliary boiler (G_{4t}) [kW] in hour t , 5) natural gas consumption by the absorption chiller (G_{6t}) [kW] in hour t , 6) natural gas consumption by the SOFC (G_{2t}) [kW] in hour t , 7) electric power from the macrogrid (U_t^{out}) [kW] in hour t , 8) electric power consumed by the VCC (P_{5t}^{in}) [kW] in hour t , 9) electric power generated by the SOFC (P_{2t}^{out}) [kW] in hour t , 10) exhaust flow from the SOFC ($\gamma_2 G_{2t}$) [kg/hr] in hour t , 11) exhaust flow from SOFC into absorption chiller (F_{6t}^{in}) [kg/hr] in hour t , 12) high-temperature exhaust flow from SOFC into boiler ($F_{3t}^{\text{in},2}$) [kg/hr] in hour t , 13) exhaust flow from absorption chiller to boiler ($F_{3t}^{\text{in},1}$) [kg/hr] in hour t , 14) cooling load provided by the absorption chiller (Q_{5t}^{out}) [kW] in hour t , 15) cooling load provided by the VCC (Q_{6t}^{out}) [kW] in hour t , 16) net flow of cold thermal energy into the CWS tank (ΔQ_t^{tank}) [kW] in hour t

4.2 System Technologies

The proposed distributed CCHP generation system flow diagram is presented in Figure 3-1. In this study, we consider the refurbishment of an existing building energy system with the installation of a new chiller and a cooling tower.

4.3 Model Description

The parameters in this model dictate the time fidelity (e.g., hourly data) and time horizon (1 hour to 8760 hours) of interest, the cooling, heating and power needs of the building, the pricing and emission rates of carbon, time-of-use and demand charges for electric power

consumption from the utility, cost of natural gas from the utility, techno-economic performance characteristics of technologies, and systems considered. In this study, all parameters are treated as deterministic.

In this study, we look at the optimal design and dispatch of CCHP systems; thus, there are separate groups of variables for design and for dispatch. Design variables determine which technologies are parts of the system and how many individual devices from each technology are installed. Many devices, such as fuel cells and chillers, can only be purchased in discrete sizes, so their associated design variables are restricted to be integer. On the other hand, cold water storage tanks can be acquired in any size and thus, for the sizing of storage tanks, integer variables are not necessary. In cases where DG technologies do not improve the objective function value, the macro-grid, the boiler, and the existing vapor compression chiller meet the energy needs of the building.

The dispatch variables determine the magnitudes and direction of the different energy flows (as seen in Figure 3-1) during each time period, e.g., how much of the waste heat from the SOFC-CHPs goes to the absorption chiller, the hot water boiler or how much is being vented. If no DG technologies are acquired, the dispatch consists of supplying the power needs through the macro-grid, the heating needs by the boiler, and the cooling needs by the macro-grid powered vapor compression chiller.

The objective of the model presented is to determine the design (sizing) and dispatch to minimize the overall costs of meeting a building's energy needs over the time horizon of interest. The total cost includes the installed costs of the technologies, the operation and maintenance costs, the costs of purchasing power and natural gas from the macro-grid, the carbon tax paid for emitted carbon by the grid as well as from fossil fuelled technologies on-site, and the revenues from net-metering. The model provides a breakdown of the costs associated with installing individual technologies and breakdown of dispatch costs (O&M, natural gas cost, demand charges, electricity charges). The model can be adjusted to give the desired output data.

In addition to the objective function, constraints are needed to model the realistic operation of a CCHP system. Constraints determine the way the different power needs are met (e.g., heating is met by the boiler, and/or waste heat from the CHP-SOFC or gradual waste heat

from the absorption chiller), restrictions imposed by the macro-grid (e.g., you cannot be a net-generator in during a year or a month), and the performance of the different technologies (e.g., the COP of the chillers), as well as how different technologies interact with each another [47].

4.4 Mathematical Formulation (\mathcal{P})

The mathematical formulation for the problem, (\mathcal{P}), is presented using the sets, parameters, and variables defined in the nomenclature. A set \mathcal{J} is defined to differentiate between technologies. The elements of the set \mathcal{J} are as follows: 2=CHP-SOFC, 4=Boiler, 5=Vapor Compression Chiller, 6=Absorption Chiller, 7=CWS tank. Detailed descriptions of the objective and constraints of (\mathcal{P}) are provided in Sections 4.4.1 through 4.4.10 [47].

4.4.1 Minimum Total Cost

The objective function minimizes the total costs for meeting the building's energy needs. The total cost includes:

- Annualized amortized capital costs of the acquired DG technologies
- Operation and maintenance costs for operating the acquired DG technologies
- Operational and maintenance costs for meeting the energy needs of the building not met by the DG (macro-grid, power cost for the VCC and natural gas cost for the boiler)
- Revenues from net-metering

$$\sum_{i \in \mathcal{J}} C_i \quad (4.1)$$

The fixed capital cost, C_1 , is the sum of all the annual amortized cost of the DG technologies acquired:

$$C_1 = \sum_{j=2,5,6} c_j k_j^{\text{out}} A_j + c_7 V_7$$

The chillers and fuel cells can be installed in discrete sizes; thus, in addition to the cost of one unit (c_j) we also need the total number of these technologies installed (A_j) as well as the size of one device (k_j^{out}). The size of a CWS tank can be increased continuously; in that case we only need the total size of the tank (V_7) and the cost per m^3 (c_7). The option to install only one type of fuel cell is given and the constraints in part 4.4.8 are used to determine if it is a power-only, CHP, CCP or CCHP system. It has to be noted that the total installed cost (c_2) is different between the power-only (\$2000/kW) and the rest of the energy systems (\$2050/kW), it also applies for the variable O&M costs (m_2) of the SOFC system. The heat recovered from the CHP-SOFC can be directed to meet the heating demand of the building and/or into a thermally activated chiller such as an absorption chiller. Waste heat can be vented at any point after the CHP-SOFCs. Because the temperature of the waste heat stream after the absorption chiller is relatively high ($\sim 170^\circ C$) it can be directed into the hot water boiler, for additional utilization, or be vented after it passes through the absorption chiller.

The initial installed cost for each of the technologies needs to be amortized for one year. In this study, capital recovery factor (CRF) is used to annualize the installed cost of equipment.

c_j = amortized initial capital cost of technology j [\$ / kWh - time horizon]

ρ = interest rate [% (fraction) per time horizon]

λ_j = average lifetime of technology j [number of time horizons]

κ_j = initial capital cost of technology j [\$ / kWh, \$ / kW, \$ / gal, or \$ / m^3]

CRF = capital recovery factor [fraction]

$$c_j = CRF \times \kappa_j$$

$$CRF = \frac{\rho(1 + \rho)^{\lambda_j}}{(1 + \rho)^{\lambda_j} - 1}$$

The variable and fixed operational costs of the DG system consist of operation and maintenance for the (CHP-)SOFCs and for the absorption and vapor compression chillers. The O&M costs, C_2 , for chillers (maintenance costs for chillers are a function of the installed capacity and the purchase price

(κ_j), ~4% (b_j) of the purchase price [33]) depends on the installed capacity and the purchase price of the equipment, the O&M of SOFC systems depend on the electric energy generated (P_{2t}^{out} times a fixed fee per kWh of power generated) because the stack of the SOFC degrades with hours in operation and needs to be replaced regularly [42]:

$$C_2 = \sum_{t \in \mathcal{T}} m_2 \delta P_{2t}^{\text{out}} + \sum_{j=5,6,7} b_j \kappa_j$$

We assume that the O&M costs for the cold-water storage tanks are fixed, and incorporated into the capital costs, as there is little need for variable maintenance (where b_j is the fraction of annual O&M cost from the total installed cost κ_j). The parameter δ is included to appropriately convert units of power (kW) to units of energy (kWh).

SOFCs operate at high temperatures, ($\sim 800^\circ\text{C}$), and they require fuel input before they are able to produce power. SOFCs also require fuel input for operation (G_{2t}). For the previous reason, the costs of emissions ($z \cdot z^g$) and fuel (g_t), C_3 , need to be taken into account. It is assumed that there is no start-up natural gas consumption for the absorption chiller. The cost of the start-up and operation of an SOFC and thermally activated chillers depends on the natural gas price (g_t) and the price of emitting carbon emissions ($z \cdot z_g$):

$$C_3 = \sum_{t \in \mathcal{T}} (g_t + z \cdot z^g) \left[\frac{\sigma_2 \mu_2 k_2}{2\eta_2^{\text{min}}} \dot{N}_{2t} + \delta G_{2t} \right] + \sum_{t \in \mathcal{T}} (g_t + z \cdot z^g) \delta G_{6t}$$

In this study, we assume that the costs of carbon emissions from the macro-grid are incorporated into the utility bill of the building operator. The amount of gas required for a single SOFC to reach operating temperature is treated as a fixed value $\left(\frac{\sigma_2 \mu_2 k_2}{2\eta_2^{\text{min}}} \right)$ which is dependent on the minimum turn-down ratio (μ_2), the minimum electrical efficiency (η_2^{min}) and the start-up time (σ_2). The variable \dot{N}_{j_t} determines how many SOFCs start up in a given time period, which allows for the calculation of the total amount of gas required. Once an SOFC reaches operating temperature, the amount of natural gas (G_{j_t}) consumed depends on the power output and the electric efficiency as defined in constraint [47] (4.5a). Natural gas consumption by the absorption chillers depends on the cooling output as well as the amount of the waste heat available from the SOFCs.

If the power-generating DG technologies are not able to meet all the building's electric power needs, or no power generating technologies are acquired in the first place, then power must be purchased from the macro-grid (U_t^{out}). In this model, the total cost of purchasing electricity, C_5 , from the macro-grid consists of the hourly rates (p_t) (per kWh) and the peak rates (p_n^{max}) (per kW of peak) charged for the monthly peak demand (U_n^{max}) as well as the carbon tax applied to the carbon emissions rate (z^p).

$$C_5 = \sum_{t \in \mathcal{T}} (p_t + z \cdot z^p) \delta U_t^{\text{out}} + \sum_{n \in \mathcal{N}} p_n^{\text{max}} U_n^{\text{max}}$$

Even though we assume that a natural gas fired boiler is installed on-site, we still need to account for its O&M, fuel, and emissions costs, C_6 :

$$C_6 = \sum_{t \in \mathcal{T}} (g_t + z z^g) \delta G_{4t}$$

The amount of natural gas (G_{4t}) consumed depends on the heating demand of the building in hour [47].

4.4.2 Power, Cooling and Heating Demand

Constraint (4.2a) ensures that the power demand of the building (d_t^P) and the vapor compression chiller (P_{5t}^{in}) is met by the power generated by the SOFC(-CHP)s (P_{2t}^{out}) and the supply from the macro-grid (U_t^{out}) in each hour. Constraint (4.2b) dictates that the natural gas-fired boiler (G_{4t}) with an efficiency of (η_4^Q), waste heat from the SOFC-CHP and residual waste heat from the absorption chiller meet the heating demand of the building (d_t^Q). The natural gas-fired boiler works with an efficiency of η_4^Q . Only a portion ($\tau_4^{\text{out}} - \tau_3^{\text{out}}$) of the waste heat from the SOFC-CHP and the absorption chiller can be utilized. Constraint (4.2c) ensures that the cooling demand (d_t^C) of the building is met by the cooling provided by the chillers ($\sum_{j=5,6} Q_{jt}^{\text{out}}$) and the net flow of cooling into the CWS tank (ΔQ_t^{tank}). Where ΔQ_t^{tank} is a negative value when the CWS tank is discharged and a positive value when the CWS tank is charged.

$$P_{2t}^{\text{out}} + U_t^{\text{out}} = d_t^P + P_{5t}^{\text{in}} \quad \forall t \in \mathcal{T} \quad (4.2a)$$

$$G_{4t}\eta_4^Q + h_3 F_{4t}^{\text{in}}(\tau_4^{\text{out}} - \tau_3^{\text{out}}) + h_3 F_{4t}^{\text{in},2}(\tau_5^{\text{out}} - \tau_3^{\text{out}}) = d_t^Q \quad \forall t \in \mathcal{T} \quad (4.2b)$$

$$\sum_{j=5,6} Q_{jt}^{\text{out}} - \Delta Q_t^{\text{tank}} = d_t^C \quad \forall t \in \mathcal{T} \quad (4.2c)$$

4.4.3 Utility Restrictions

Constraint (4.3a) determines the monthly billable peak power load (U_n^{max}), which is the largest hourly average load supplied by the grid in that month (U_t^{out}).

$$U_n^{\text{max}} \geq U_t^{\text{out}} \quad \forall n \in \mathcal{N}, t \in \mathcal{T}_n \quad (4.3a)$$

4.4.4 Power and Cooling Capacity

Due to its high operating temperature, the SOFCs cannot operate from a part load ratio of 0 to a part load ratio of 1 (the design output); the same applies both of the chillers types. Constraint (4.4a) enables to set the minimum turn-down ratio (μ_j) of SOFCs and chillers relative to the installed capacity of the individual devices. Constraint (4.4b) ensures that the number of fuel cells or chillers working in each hour (N_{jt}) cannot exceed the overall number of fuel cells or chillers installed (A_j).

$$\mu_j k_j^{\text{out}} N_{jt} \leq P_{jt}^{\text{out}} \leq k_j^{\text{out}} N_{jt} \quad \forall j = 2, 5, 6, 7 \quad t \in \mathcal{T} \quad (4.4a)$$

$$N_{jt} \leq A_j \quad \forall j = 2, 5, 6, 7 \quad t \in \mathcal{T} \quad (4.4b)$$

4.4.5 Electric Efficiency

Constraint (4.5a) demonstrates that the average electrical efficiency (E_{jt}) of an SOFC in hour t is a function of the part load ratio ($\frac{P_{jt}^{\text{out}}}{N_{jt}k_j^{\text{out}}}$) occurring in that hour. SOFCs operate between the maximum (η_j^{max}) and minimum (η_j^{min}) pre-determined efficiencies.

$$E_{jt} = \eta_j^{\max} - \left(\frac{\eta_j^{\max} - \eta_j^{\min}}{k_j^{\text{out}}} \right) \left(\frac{P_{jt}^{\text{out}}}{N_{jt}} \right) \quad \forall j = 2, t \in \mathcal{T} \quad (4.5a)$$

4.4.6 Natural Gas and Power Consumption

Constraint (4.6a) determines that the natural gas consumed by both power-only (G_{1t}) and CHP-SOFCs (G_{2t}) during a time period is equal to the ratio of the electric power generated (P_{jt}^{out}) over the variable efficiency (E_{jt}) during that time period (hour). In constraint (4.6b), the natural gas consumed by the absorption chiller (G_{6t}) over time period t is equal to the ratio of cooling output from the chiller during that time period (Q_{6t}^{out}) over the COP of the chiller (COP_6) less the share of waste heat that could be utilized during that time period, where F_{6t}^{in} indicates the mass flow-rate of waste heat into the absorption chiller, h_3 the specific heat of waste heat, η_j^Q the efficiency of the heat exchange and $\tau_6^{\text{in}} - \tau_6^{\text{out}}$ the difference of the waste heat temperature between before and after going through the absorption chiller. Constraint (4.6c) shows that the electric power consumed by the vapor compression chiller (P_{5t}^{in}) over a time period is equal to the ratio of the cooling provided (heat removed from the building) (Q_{5t}^{out}) over the COP value of the chiller (COP_5).

$$G_{jt} = \frac{P_{jt}^{\text{out}}}{E_{jt}} \quad \forall j = 2, t \in \mathcal{T} \quad (4.6a)$$

$$G_{6t} + \delta \eta_j^Q h_3 F_{6t}^{\text{in}} (\tau_6^{\text{in}} - \tau_6^{\text{out}}) = \frac{Q_{6t}^{\text{out}}}{COP_6} \quad (4.6b)$$

$$P_{5t}^{\text{in}} = \frac{Q_{5t}^{\text{out}}}{COP_5} \quad \forall t \in \mathcal{T} \quad (4.6c)$$

4.4.7 Start-Up and Ramping of SOFC(-CHP)s

As SOFCs, both power-only and CHP, require time and energy for start-up, it is necessary to find out how many SOFCs are being turned on and off in each hour and constraint (4.7a) establishes the number of SOFCs that start-up between time periods t and $t + 1$. If $\dot{N}_{j,t+1}$ is a positive number then it will appear in the objective function. As the objective function

minimizes the overall costs then a low number of start-ups are desirable. Constraint (4.7b) indicates that the increase or decrease of power output from SOFCs cannot exceed the total ramping capacities determined (r_j^{up} and r_j^{down}). The parameter δ converts units from kW/hr to kW .

$$N_{j,t+1} - N_{jt} \leq \dot{N}_{j,t+1} \quad \forall j = 2, t < |\mathcal{T}| \quad (4.7a)$$

$$-\delta r_j^{\text{down}} N_{jt} \leq P_{j,t+1}^{\text{out}} - P_{jt}^{\text{out}} \leq \delta r_j^{\text{up}} N_{j,t+1} \quad \forall j = 2, t < |\mathcal{T}| \quad (4.7b)$$

4.4.8 Heat Capacity

SOFCs operate at high temperatures; thus, the waste heat from them is high grade. Constraint (4.8a) determines the mass flow-rate of available exhaust ($\gamma_2 G_{2t}$) and allows splitting the exhaust flow between the absorption chiller (F_{6t}^{in}) and the heating demand (F_{3t}^{in}). Not all of the waste heat needs to be utilized (thus the " \leq "), some or all of the waste heat can be vented after the SOFC. Constraint (4.8b) indicates that the exhaust flow exiting the absorption chiller can be utilized further for meeting the heating demand ($F_{3t}^{\text{in},2}$) or it can be partially or fully vented after being utilized by the absorption chiller. The binary values (parameters), on the right hand side of the equations shown below, are used to switch between power-only, CHP, CCP and CCHP energy systems. We need additional constraints to be able to switch off exhaust flows to the absorption chiller (F_{6t}^{in}) and hot water boiler (F_{3t}^{in}) individually. Constraint (4.8c) says that the exhaust flow rate into the absorption chiller cannot be higher than the total available exhaust flow ($\gamma_2 G_{2t}$). Constraint (4.8d) says that the exhaust flow rate into the hot water boiler cannot be higher than the total available exhaust flow ($\gamma_2 G_{2t}$).

$$F_{3t}^{\text{in}} + F_{6t}^{\text{in}} \leq \gamma_2 G_{2t} b^{\text{CCHP}} \quad \forall t \leq \mathcal{T} \quad (4.8a)$$

$$F_{3t}^{\text{in},2} \leq F_{6t}^{\text{in}} b^{\text{CCHP},2} \quad \forall t \leq \mathcal{T} \quad (4.8b)$$

$$F_{3t}^{\text{in}} \leq \gamma_2 G_{2t} b^{\text{CHP}} \quad \forall t \leq \mathcal{T} \quad (4.8c)$$

$$F_{6t}^{\text{in}} \leq \gamma_2 G_{2t} b^{\text{CCP}} \quad \forall t \leq \mathcal{T} \quad (4.8d)$$

In Table 4-1, the values of the binary parameters are presented to switch between CHP, CCP and CCHP. In order to have a power-only SOFC, all of those binary parameters have to have a value of 0.

Table 4-1: SOFC waste heat utilization matrix

	Power-only	CHP	CCP	CCHP, 1	CCHP, 2
B^{CHP}	0	1	0	1	0
B^{CCP}	0	0	1	1	1
B^{CCHP}	0	1	1	1	1
$B^{CCHP,2}$	0	0	0	0 (1)	1

In Table 4-1, in the “CCHP, 1” column the parameter values $b^{CCHP,2}$ can be assigned a value 0 or 1 by the model user, depending on if the residual waste heat from the absorption chiller is vented ($b^{CCHP,2} = 0$) or utilized further for space heating ($b^{CCHP,2} = 1$) entirely or partially. In the power-only case all of the waste heat is vented. In the “CHP” case the waste heat can be used entirely or partially for space heating by directing the waste heat entirely or partially into the boiler. In the “CCP” case the waste heat can be used entirely or partially for cooling, by directing the available heat into the absorption chiller. In the “CCHP, 2” case the waste heat is first directed into the absorption chiller and then the waste heat can further be used for heating. Again, the available waste heat can be utilized entirely or partially in both steps.

4.4.9 Cold Thermal Storage

Constraint (4.9.a) determines the energy balance of the CWS tank. The net cooling rate from the tank is equal to the difference between the cold thermal energy stored under the thermocline in hour t and in hour $t + 1$. The amount of cold thermal energy stored in hour t is reduced by the fraction $\frac{\alpha}{24}$ to account for heat gains from the environment. Constraint (4.9b) ensures that the maximum cold thermal energy stored in the CWS tank (Q_t^{tank}) is less than or equal to the total capacity of the CWS tank (\bar{Q}^{tank}). Constraint (4.9c) estimates the volume of the CWS from the total thermal capacity of the CWS tank.

$$Q_{7,t+1}^{\text{tank}} - Q_{7t}^{\text{tank}} \left(1 + \frac{\alpha}{24}\right) = \Delta Q_{7t}^{\text{tank}} \quad \forall t \in \mathcal{T} \quad (4.9a)$$

$$\bar{Q}_7^{\text{tank}} \geq Q_{7t}^{\text{tank}} \quad \forall t \in \mathcal{T} \quad (4.9b)$$

$$\bar{V}_7^{\text{tank}} = \frac{\bar{Q}_7^{\text{tank}}}{c^p \beta \rho (\tau_a - \tau_b)} \quad \forall t \in \mathcal{T} \quad (4.9c)$$

4.4.10 Non-negativity and integrality

Constraints (4.10a - 4.10d) dictate which variables are non-negative. Devices, like fuel cells, come in fixed sizes, constraints (4.10c) and (4.10d) show that the number of those devices comes in integer values.

$$E_{jt}, F_{jt}^{\text{out}}, F_{jt}^{\text{in}}, G_{jt}, N_{jt}, \dot{N}_{jt}, P_{jt}^{\text{in}}, P_{jt}^{\text{out}}, Q_{jt}, Q_{jt}^{\text{in}}, Q_{jt}^{\text{out}}, T_{jt}, V_j \geq 0 \quad \forall j \in \mathcal{J}, t \in \mathcal{T} \quad (4.10a)$$

$$U_t^{\text{out}}, U_n^{\text{max}} \geq 0 \quad \forall n \in \mathcal{N}, t \in \mathcal{T} \quad (4.10b)$$

$$A_j, N_{jt} \geq 0, \text{ integer} \quad \forall j \neq 7, t \in \mathcal{T} \quad (4.10c)$$

$$A_j \text{ binary} \quad \forall j = 7, t \in \mathcal{T} \quad (4.10d)$$

4.5 Solution techniques

According to [47], optimization algorithms capable of solving linear approximations of large, nonconvex MINLPs, such as (\mathcal{P}) , are limited and dependent on the problem structure. A traditional method called branch-and-bound is not capable of solving (\mathcal{P}) presented at the beginning of this chapter; however, branch-and-bound algorithms are capable of solving linear approximations of MINLPs like (\mathcal{P}) . A branch-and-bound algorithm requires methods to obtain global lower and upper bounds on the objective value at each node, in order to converge at the optimal solution. In [47], methods to obtain those lower and upper bounds for each hour were developed, namely, a lower bounding method, (\mathcal{U}) , and an upper-bounding method, (\mathcal{H}) , that are used to bound and solve the linear approximation of (\mathcal{P}) .

4.5.1 Mathematical Structure

The mathematical structure of the solution techniques used to solve the large, nonconvex MINLP at hand was developed and explained in [47]. Here, a summary of the approach is presented. Nonlinear constraints (4.5a) and (4.6a) are rearranged, and by suppressing the linear terms, we can see that all the nonlinearities in (\mathcal{P}) consist of bilinear terms in equality constraints (see below). Thus, the constraint set is nonconvex.

$$\text{Linear} + N_{jt}E_{jt} = 0$$

$$\text{Linear} + G_{jt}E_{jt} = 0$$

In branch-and-bound, global upper bounds for MILPs are provided by integer-feasible solutions obtained with local solvers and global lower bounds are provided by solutions to continuous relaxations of the integer problem. Those bounds are hard to obtain for the problem at hand, (\mathcal{P}) , which is a large and nonconvex MINLP. Methods developed by [47] to obtain those upper and lower bounds are introduced in the following sections.

4.5.1.1 Lower Bounding: Convex Underestimation (\mathcal{U})

For a minimization problem, relaxing the integrality restrictions and solving the resulting continuous problem enables us to obtain a lower bound for a mixed-integer linear programming (MILP) problem. A lower bound for a convex MINLP can be obtained in a similar fashion. Nonconvex problems give no guarantee of a global lower bound when solving a NLP relaxation.

According to equations (3) and (4) of [2], bilinear terms are underestimated by their convex envelope. The convex envelopes are constructed by replacing each of the nonlinear terms with new variables and adding linear inequality constraints that bound the new variable. Bilinear terms require four constraints on the new variable. Considering our nonlinear terms from the constraints in (\mathcal{P}) it contains $2|\mathcal{T}| - 1$ distinct bilinear terms that must be replaced with new variables. Accordingly, the (\mathcal{U}) formulation is identical to (\mathcal{P}) with the exceptions of adding $2|\mathcal{T}| - 1$ new continuous variables, replacing each of the bilinear terms with the appropriate new continuous variable, and adding $8|\mathcal{T}| - 4$ new linear constraints. Hence, (\mathcal{U}) is an MILP, the

solution to which provides a global lower bound on the optimal solution to (\mathcal{P}) [47]. The formulation of the convex envelopes in (\mathcal{U}) requires the following upper and lower bounds on each of the original variables in the bilinear terms [47]:

Variable bounds applied in (\mathcal{U})

$$0 \leq N_{jt} \leq \left\lceil \frac{\max_{t \in \mathcal{T}}\{d_t^P\} + \max_{t \in \mathcal{T}}\{d_t^C\}/COP_5}{k_j^{\text{out}}} \right\rceil$$

$$0 \leq G_{jt} \leq \left(\frac{k_j^{\text{out}}}{\eta_j^{\text{min}}} \right) \left\lceil \frac{\max_{t \in \mathcal{T}}\{d_t^P\} + \max_{t \in \mathcal{T}}\{d_t^C\}/COP_5}{k_j^{\text{out}}} \right\rceil$$

$$0 \leq F_{3t}^{\text{in}} + F_{6t}^{\text{in}} \leq \gamma_2 \left(\frac{k_2^{\text{out}}}{\eta_2^{\text{min}}} \right) \left\lceil \frac{\max_{t \in \mathcal{T}}\{d_t^P\} + \max_{t \in \mathcal{T}}\{d_t^C\}/COP_5}{k_2^{\text{out}}} \right\rceil$$

$$\eta_j^{\text{min}} \leq E_{jt} \leq \eta_j^{\text{max}}$$

The upper bound on the number of SOFCs operating in hour t (N_{jt}) is determined by the sum of the maximum non-AC electrical peak of the time period and the maximum electric load of the annual cooling peak met with a VCC. By summing those two peaks, the upper bound is overestimated, as the non-AC peak and the cooling peak are not coincident. An overestimated (relaxed) upper bound does not create problems in finding a solution. The upper bound for the natural gas consumption by the SOFC in hour t (G_{jt}) is found in a similar fashion. However, the upper bound of the natural gas consumption by the SOFC in hour t is dependent on the minimum electrical efficiency (η_j^{min}) of the SOFC, rather than the size of an individual SOFC (k_j^{out}). The electrical efficiency of the SOFC in hour t is between the predetermined values of η_j^{min} and η_j^{max} . The maximum flowrate of CHP-SOFC ($F_{3t}^{\text{in}} + F_{6t}^{\text{in}}$) exhaust is obtained from equation 4.8a.

4.5.1.2 Upper Bounding: Linearization Heuristic (\mathcal{H})

A linearization heuristic, (\mathcal{H}), is presented, for determining integer-feasible solutions to (\mathcal{P}) that can be applied to the large instances considered in this study. The formulation of the linearization heuristic problem (\mathcal{H}) is identical to the nonlinear problem (\mathcal{P}). Fixing the value for (E_{jt}) linearizes the nonlinearities of (\mathcal{P}). The (\mathcal{P}) feasible solution algorithm is presented below. First, the convex underestimation problem (\mathcal{U}) is solved, and values for the power generated by the SOFCs or the CHP-SOFCs in hour t ($\check{P}_{1t}^{\text{out}}$) and the number of SOFCs or CHP-SOFCs operating in hour t (\check{N}_{1t}) $\forall t$ are obtained. Both $\check{P}_{1t}^{\text{out}}$ and \check{N}_{1t} are used in step 2) to calculate the fixed value of (E_{jt}). Also, if the number of SOFCs or CHP-SOFCs in a particular hour is 0 ($N_{1t} = 0$), then the lowest efficiency η_1^{min} is assigned to the prime mover to dividing with 0 in the model. After obtaining a value for E_{jt} , the heuristic problem (\mathcal{H}) can be solved. By solving the heuristic problem (\mathcal{H}), values for the design and dispatch variables are obtained, as well as an objective function value.

(\mathcal{P})-feasible Solution Algorithm

- 1) Solve (\mathcal{U}) and store resulting values for $\check{P}_{1t}^{\text{out}}$ and \check{N}_{1t} $\forall t$.
- 2) Set

$$E_{1t} = \check{E}_{1t} = \eta_1^{\text{max}} - \left(\frac{\eta_1^{\text{max}} - \eta_1^{\text{min}}}{k_1^{\text{out}}} \right) (\check{P}_{1t}^{\text{out}} / \check{N}_{1t}) \text{ if } N_{1t} > 0, \eta_1^{\text{min}} \text{ otherwise } \forall t.$$

- 3) Solve (\mathcal{H}) and return its solution

Table 4-2: Summary of optimization runs

Sensitivity Analysis				
Sensitivity Parameter	Range [unit]	Building Type	Location	Equipment/Installed Cost
VCC COP	$\pm 25\%$	Medium Office Large Hotel	SF Boston	VCC only VCC+CWS
CO ₂ Tax	20 and 60 [\$/ton _{CO₂}]	Large Hotel	SF Boston	VCC+ABS VCC: 370 [\$/kW] (105 [\$/ton]) ABS: 754 [\$/kW] (210 [\$/ton])
Individual Technologies and Energy Systems				
Technology/Energy System	Building Type	Location	System Configuration/ Installed Cost	
VCC (baseline)	Medium Office Large Hotel	SF Boston	VCC VCC: 370 [\$/kW] (105 [\$/ton])	
ABS	Medium Office Large Hotel	SF Boston	VCC+ABS VCC: 370 [\$/kW] (105 [\$/ton]) ABS: 754 [\$/kW] (210 [\$/ton])	
Cold Water Storage Tank	Medium Office Large Hotel	SF Boston	VCC+CWS VCC: 370 [\$/kW] (105 [\$/ton]) CWS: 280 [\$/m ³]	

4.6 Summary of optimization runs

In Table 4-2, the planned optimization runs are presented. We will perform sensitivity analysis on tax on CO₂ emissions and the COP of the VCC. The purpose of running sensitivity analysis on CO₂ tax is to find what, and if any, effect it has on the total cost and system design. The COP of the VCC is investigated because in Section 3.2 we saw that it has a significant impact on the energy consumption of the VCC. We also look at how absorption chillers and CWS tanks perform compared to the baseline case where only a VCC is installed during the refurbishment of the building energy system.

CHAPTER 5

RESULTS AND DISCUSSION

The model and techniques developed in earlier chapters are used to investigate multi-energy generation systems with and without thermal energy storage at two locations and with two different building types.

First, the cost breakdown of the baseline case (only a VCC is installed) by end use (cooling, heating, power and amortized cost) and cost type (demand charges, natural gas consumption, energy charges and amortized cost) is presented.

Secondly, sensitivity analysis is performed on the effects of the chiller COP and a tax on CO₂ emissions on the total annual costs and the cooling sub-system. The range at which the parameters are varied in the sensitivity analysis is presented in Table 4-2.

Next, we take a closer look at the CWS and absorption chiller technologies to determine what makes it generate savings for the building owner (e.g., why does a combination of absorption and VCC chillers offer savings to the building operator, compared to a VCC only system). It is desirable to understand the magnitude of the savings, the associated underlying reasons for such economic benefit, and the range of conditions for which savings can be realized. Thus, the following comparisons of total annual savings and simple payback times are presented.

5.1 Existing Building Energy System

In the baseline case (VCC only), the cost of equipment indicates the annualized cost of obtaining the VCC to meet the building cooling demand. In Figure 5-1, it can be seen that the cost breakdown by end use for different building types and locations varies significantly. The cost of heating in a medium sized office building is about three times less than the cost of heating in a large hotel. From that, we can predict that the CHP capability benefits an SOFC more in a

large hotel because a larger fraction of waste heat can be utilized to offset natural gas consumption of the auxiliary boiler.

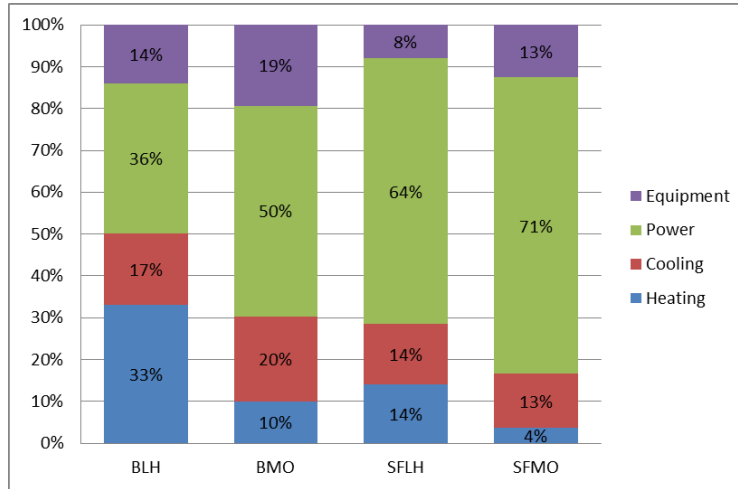


Figure 5-1: Breakdown of total annual cost by end use

*System: Baseline - Vapor Compression Chiller only, Equipment cost – annualized total installed cost

When SOFC(-CHP) is installed on site, it becomes impossible to differentiate what share of power purchased from the utility and generated on-site goes for meeting the cooling demand and what share goes to meet the general power demand. Figure 5-2 presents the cost breakdown by cost type of the baseline building energy system.

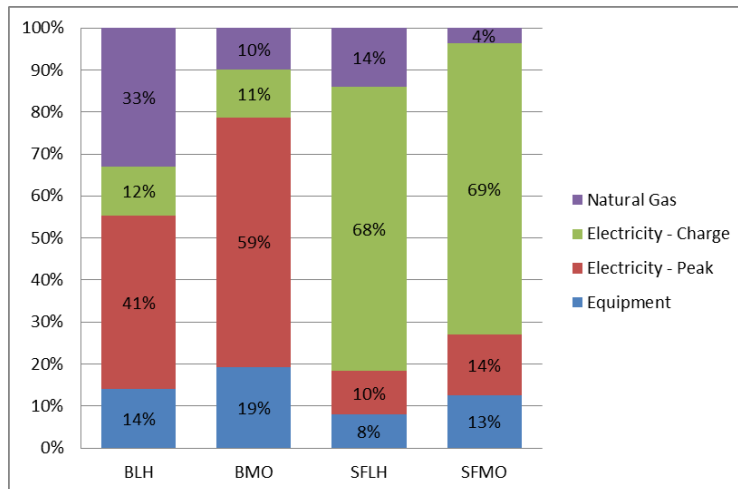


Figure 5-2: Breakdown of total annual cost by cost type

*System: Baseline - Vapor Compression Chiller only

The electricity bills differ greatly between Boston and San Francisco. In Boston, peak demand charges dominate the total annual cost and in San Francisco electricity charges dominate the total annual cost.

5.2 Simple payback time (SPT)

An important factor in making a decision to install DG systems on-site is the payback period of the installed system. Simple payback time (SPT) is calculated as follows:

$$SPT = \frac{\text{Total Installed Cost}}{\text{Total Annual Savings}} = \frac{\text{Proposed}_{TIC} - \text{Baseline}_{TIC}}{\text{Baseline}_{TAS} - \text{Proposed}_{TAS}}$$

In this study, the total installed cost of the baseline system (Baseline_{TIC}) is the total installed cost of a VCC system. The total cost of the proposed system (Proposed_{TIC}) is the total installed cost of the system e.g. an SOFC+VCC system.

5.3 Effects of chiller COP

Recall that the method for estimating COP values for VCC and absorption chiller hardware was given in Section 3.3; in this research effort, the COP values are fixed. While the MINLP approach assumes a fixed value for chiller COP, in reality, COP values are not fixed and thus it is important to evaluate what effect different values have on the design, dispatch and the total cost of the building energy system. Average COP values from Table 5-1 are altered by $\pm 25\%$ for a large hotel in Boston and the following system configurations are considered: VCC and VCC+CWS. The system configurations and the change in total cost are illustrated in Table 5-1.

Table 5-1 indicates that the change in the COP by $\pm 25\%$ results in a 3 to 5% change, respectively, in the total system cost for a large hotel in Boston. With the absence of other technologies like CWS and SOFCs, varying the COP of the VCC changes the total annual cost by 3 to 5% CWS tanks already decrease the overall cost, thus, the effect of changing the COP on cost is diminished as it is altered by only 1 to 1.8%.

Regarding design, the size of the CWS is most affected by the change in the COP value. The size of CWS decreases with an increasing COP; this is because there is less incentive to store chilled water when a high efficiency chiller is used to produce chilled water and fewer savings are achieved from CWS.

Table 5-1: Effects of changing the COP of VCC by $\pm 25\%$ on total annual cost

	System Configuration	VCC [kW] (ton)	SOFC [kW]	CWS [m³]	Change in Total Annual Cost [%]
Boston/Large Hotel	VCC(COP -25%)	800 (227)	0	0	-5.15%
	VCC	800 (227)	0	0	N/A
	VCC(COP +25%)	800 (227)	0	0	3.00%
	VCC(COP -25%)+CWS	570 (162)	0	265	-1.79%
	VCC+CWS	580 (164)	0	224	N/A
	VCC(COP +25%)+CWS	550 (156)	0	220	1.06%

Results indicate that the COP value has an impact on both the design and total cost of a multi-energy generation building energy system. However, a significant alteration of the COP value results in only a minor change in the objective function value and the system design. Altering the COP by $\pm 25\%$ can change the size of the CWS by $\pm 20\%$ (when the size of the VCC is fixed). The small impact of different COP values on the overall costs results because cooling contributes only up to 20% of the total cost of meeting the cooling, heating, and power needs of a building. Since the CWS is a part of the cooling sub-system of the building, varying the COP has a significant impact on the size and dispatch of the CWS.

5.4 Switch Points and Sensitivity Analysis

Absorption chillers become economically unattractive when a CWS tank is installed, we determine the total installed cost necessary to make absorption chillers competitive when a CWS tank is installed onsite.

5.4.1 Absorption chillers

In Boston, when using a cooling system combining VCC and absorption chillers, the absorption chillers perform peak shaving by using natural gas to provide cooling. However, due to the high-energy charges in San Francisco, absorption chillers meet the cooling baseload and a VCC is used to meet the daily cooling peaks. Absorption chillers become unattractive when used in combination with CWS, since CWS systems can perform peak shaving and load shifting at a lower cost compared to absorption chillers. In order for an absorption chiller to be able to compete with CWS tanks, the total installed cost of the absorption chiller needs to be reduced (see Table 5-2).

Table 5-2: % reduction in total installed cost required for the absorption chiller

System Configuration	San Francisco, LH [\$/kW-yr]	San Francisco, MO [\$/kW-yr]	Boston, LH [\$/kW-yr]	Boston, MO [\$/kW-yr]
VCC+ABS+CWS	745 (-24%)	520 (-47%)	575 (-41%)	690 (-29%)

The threshold values in Table 5-2 indicate the total installed cost of absorption chillers where absorption chillers can compete with CWS tanks. Table 5-2 indicates that significant total installed cost reductions in the range of 24%-47% are required.

5.4.2 Tax on carbon dioxide emissions

In recent years, there have been rising concerns about the impact of power conversion on the environment. As a way to motivate the industry to invest in environmentally benign technologies, there is a debate about implementing a tax on CO₂ emissions. The following tax

rates on CO₂ emissions are investigated: \$20/ton and \$60/ton of CO₂. A tax of \$60/ton is considered high and a tax of \$20/ton of CO₂ moderate. In this study, we want to investigate the effects of a tax on CO₂ emissions on the design, dispatch and total cost of buildings in different locations. A system configuration with VCC and absorption chillers is investigated for a large hotel in Boston and San Francisco.

Results indicate that a carbon tax in Boston favors technologies running on natural gas (see Table 5-3) and in San Francisco a carbon tax benefits the macro-grid and the use of VCC. Results also indicate that a carbon tax of \$20/ton in Boston has the potential of increasing the total cost by 15%, while in San Francisco the same carbon tax rate increases the total cost only by 8%. That trend is explained by the fact that grid emissions in Boston are higher compared to grid emissions in San Francisco.

Table 5-3: Sensitivity analysis of CO₂ tax in Boston

Large Hotel, Boston	VCC [kW]	ABS [kW]	Change in Total Annual Cost
No tax	510	290	N/A
\$20/ton	470	340	15%
\$60/ton	470	340	50%

5.5 Addition of an Absorption Chiller

Absorption chillers are an alternative to vapor compression chillers; they use only a fraction of the electric energy of vapor compression chillers. This reduced electric power consumption is due the fact that a liquid is compressed instead of a vapor. We conducted optimization runs with the option to install both VCCs and/or absorption chillers; the results are presented in Table 5-4. The VCC only option in Table 5-4 (and the tables below) indicates the size of the VCC for the baseline system configuration, when only a VCC is installed. This study looks at either new buildings or retrofit projects where the existing chiller as well as its cooling

tower are at the end of their lives and need to be replaced. In Table 5-4, the VCC and ABS sizes, in the second and third row respectively, indicate the sizes of the chiller when both VCC and ABS chillers would be installed. The installation of absorption chillers alone results in an increased total annual cost compared to the baseline cost (VCC only) and, thus, is not presented. However, the installation of both VCC and absorption chillers will result in savings of 0.7 to 1.5%. The installation of absorption chillers will also result in increased CO₂ emissions, at least in San Francisco and Boston.

Table 5-4: Installation of absorption chillers

	Boston		San Francisco	
	Large Hotel	Medium Office	Large Hotel	Medium Office
VCC only (baseline) [kW] (ton)	800 (227)	290 (82)	440 (125)	190 (54)
VCC [kW] (ton)	510 (145)	200 (57)	290 (82)	140 (40)
ABS [kW] (ton)	290 (82)	90 (25)	150 (43)	50 (14)
Change in Total Annual Cost [%]	-1.53%	-1.33%	-3.08%	-0.68%
ΔCO_2 emissions [%]	0.48%	0.47%	5.63%	5.64%
Simple Payback Time [years]	7.2	7.7	4.3	7.8

The increased CO₂ emissions are due to the increased consumption of natural gas at low COP values, ~1.2 for an absorption chiller, versus ~4 for a VCC. Due to increased concerns about climate change, there has been more discussion about a tax on CO₂ emissions. Applying a CO₂ tax of \$20/ton_{CO₂}, increases the installed capacity of the VCC by 10-20kW at both locations, and reduces the installed capacity of the absorption chiller by the same amount.

Figure 5-3 demonstrates a reduction in the share of demand charges in Boston (6-7%), and a reduction in the share of cost of electricity charges in San Francisco (5-8%). At the same time, the annualized installed cost and the natural gas bill increase, resulting in small total annual savings (0.7-3.08%) and relatively long payback times (4.3-7.8 years).

5.5.1 Dispatch for VCC and absorption chiller system

In order to investigate how dispatch strategies differ between Boston and San Francisco, San Francisco utility pricing structure is applied to the demand profiles of a large hotel in Boston. The goal is to differentiate between the effects of utility pricing and the effects of local climate on the design and dispatch of a DG system.

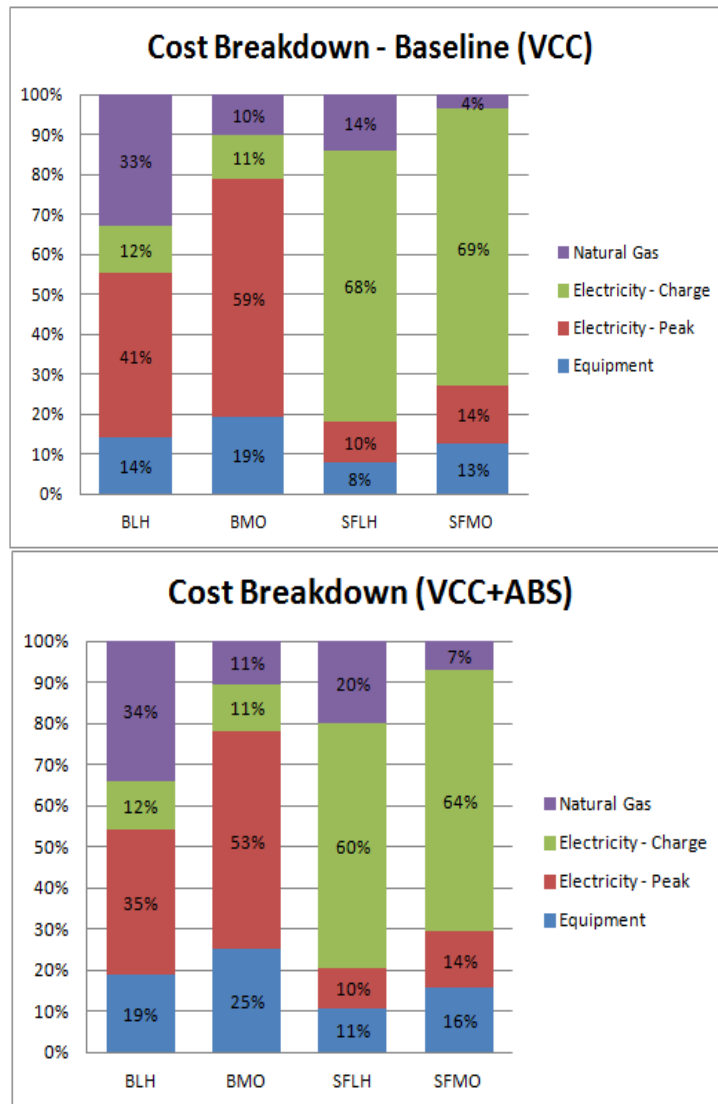


Figure 5-3: Cost breakdown comparison (VCC vs. VCC+ABS)

In San Francisco, on the other hand the absorption chiller runs constantly and the VCC is turned on when the full capacity of the absorption chiller is reached. In San Francisco, the absorption chiller can utilize cheap natural gas instead of expensive power to provide cooling.

However, the absorption chiller needs to run at high capacity factors in order to sustain competitiveness (high installed cost), and because of that a VCC is used for meeting the cooling peaks. In this study we let the optimization model decide what size the installed devices are, and thus, it is not known if reducing the size of the absorption chiller would improve its economics. However, when the size of the absorption chiller is decreased the size of the size of the VCC is increased and the economics of the building system might hurt because more, relatively expensive, electric power is used to provide cooling.

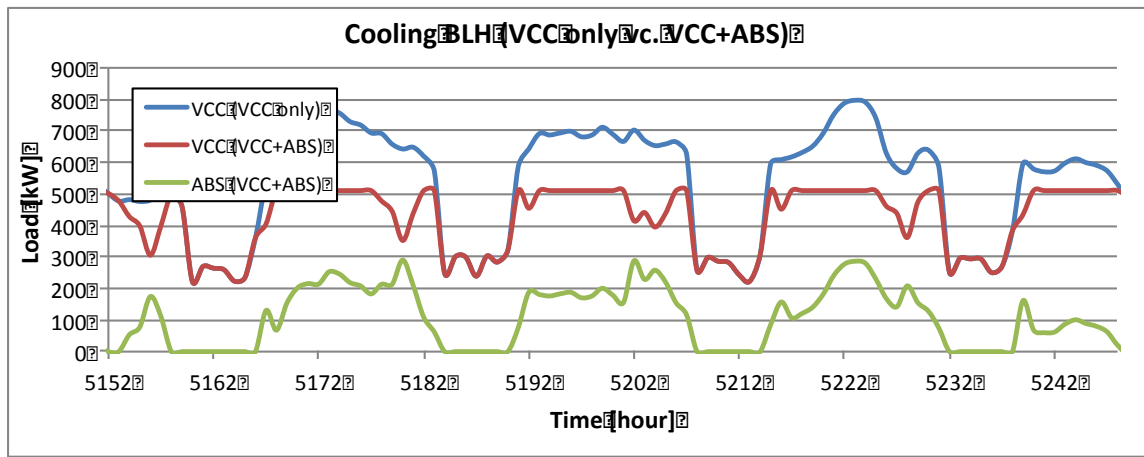


Figure 5-4: Chiller operation between VCC and VCC+ABS systems (Large Hotel in Boston)

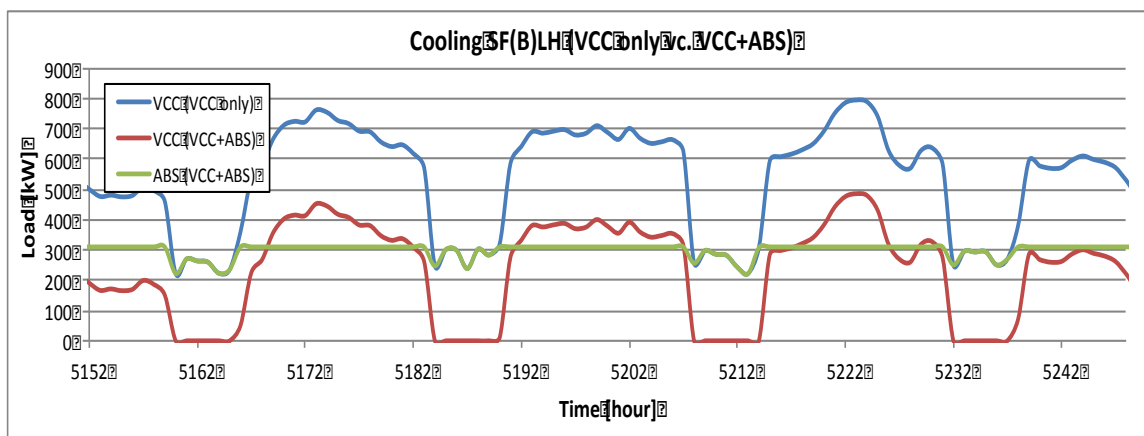


Figure 5-5: Chiller operation (VCC vs. VCC+ABS) (San Francisco utility pricing – with Boston load profiles)

5.6 Addition of Chilled Water Storage (CWS) Tank

A building operator can benefit from the installation of a CWS tank through reduced chiller size and flexibility towards utility pricing structures (load shaving and load shifting). CWS tanks can be integrated into an existing chilled water-cooling system without major modifications to that cooling system and the cooling equipment. We conduct optimization runs where the option to install VCCs and/or absorption chillers and CWS tanks is present.

Table 5-5: Installation of a CWS tank

	Boston		San Francisco	
	Large Hotel	Medium Office	Large Hotel	Medium Office
VCC only [kW] (ton)	800 (227)	290 (82)	440 (125)	190 (54)
VCC [kW] (ton)	580 (164)	160 (45)	230 (65)	80 (23)
CWS [m ³]	223.968	117.899	109.6	69.8881
Change in Total Annual Cost [%]	-10.83%	-16.08%	-7.08%	-10.74%
ΔCO_2 emissions [%]	-2.63%	-1.54%	-2.31%	-3.93%
Simple Payback Time [years]	0*	0*	0*	0*

*indicates that the capital costs are lower compared to the baseline case, as the installation of CWS reduces the size of a VCC

None of the locations and building types choose absorption chiller at the presence of CWS tanks; because, at the presence of a CWS tank the COP of a VCC is increased resulting in an improved economic performance of the VCC device. These results are presented in Table 5-5. Table 5-5 indicates that by installing a CWS tank, a building owner can reduce the total annual cost by 7 to 16% compared to the baseline case (VCC only). A medium-sized office in Boston has the highest savings potential (~16%). The higher savings potential of CWS tanks in a medium-sized office can be credited to the fact that both peak-shaving and load shifting potential is higher in a medium-sized office compared to a large hotel due to the significant difference between daily peak and minimum power demands.

In addition to reducing the total annual cost, a CWS tank reduces CO₂ emissions. The decline in CO₂ is due to the fact that at the presence of a CWS tank chillers operate at higher CF

and thus, higher COP values (lowering primary energy consumption). Figure 5-6 shows the cost breakdown by cost type. In Boston the total annual savings are mostly due to reduced peak demand charges and in San Francisco due to reduced capital costs.

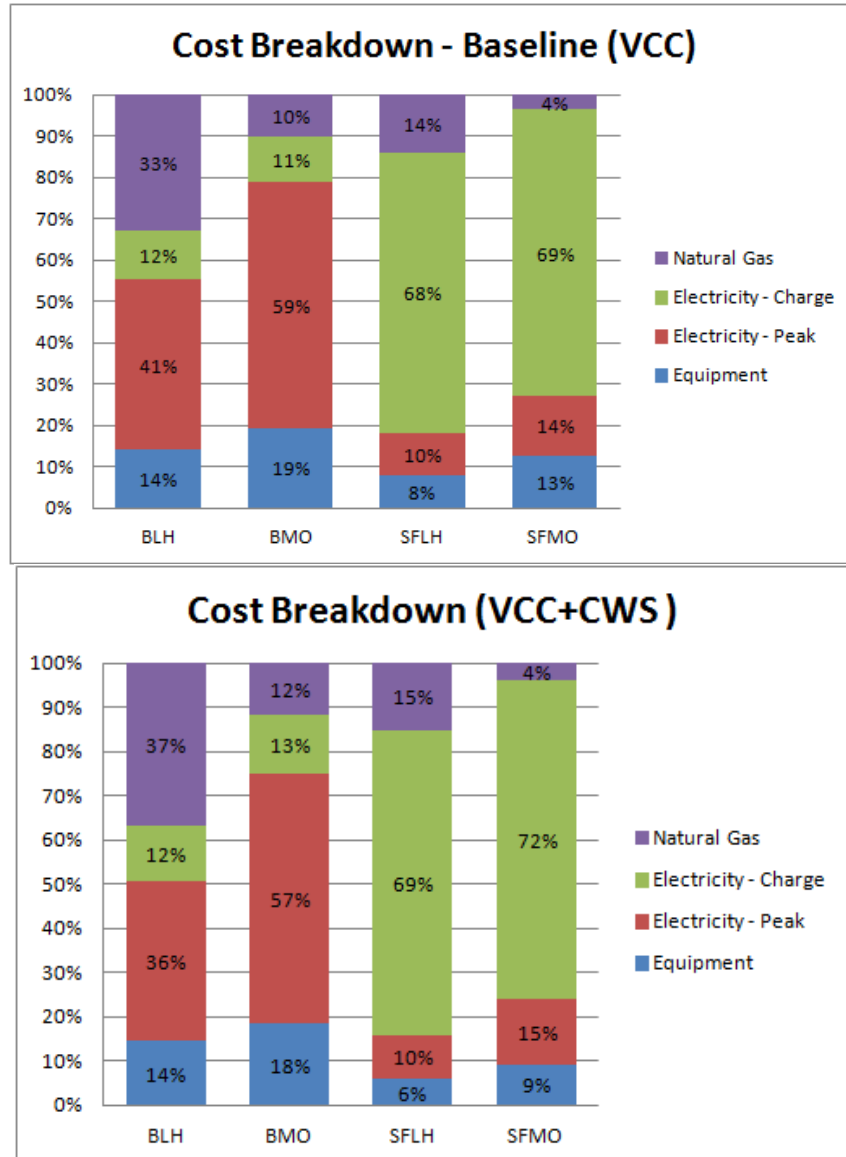


Figure 5-6: Cost breakdown (VCC vs. VCC+CWS)

Compared to a large hotel, savings of 4 - 6 percentage points higher can be achieved in medium sized offices. The increased savings in medium sized office buildings is due to the nature of the building load profiles. The day-to-day and hourly load variability is significantly higher in a medium-sized office compared to a large hotel (see Table 3-4); thus, load shifting and peak shaving have a more dramatic impact on the total cost savings in medium-sized offices. In

addition, the installation of CWS in a medium sized office building will increase the COP of a VCC by a larger margin compared to a large hotel (see Table 5-5).

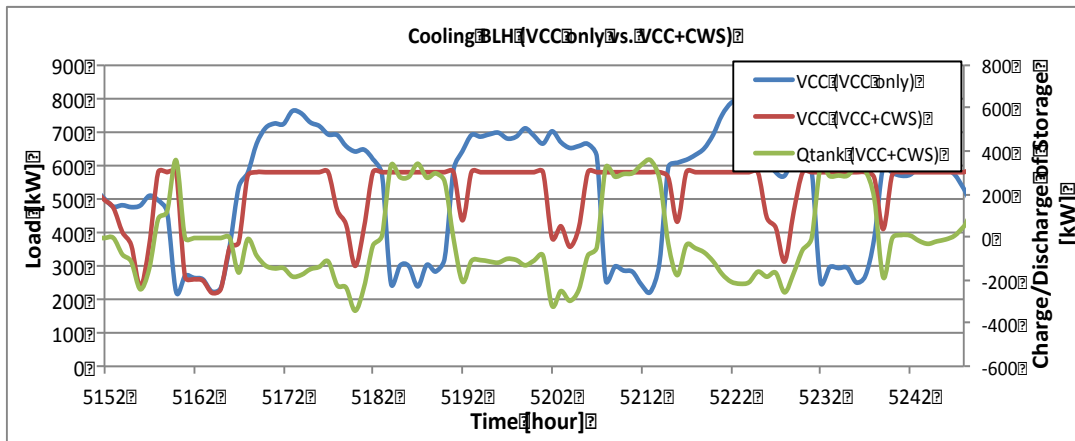


Figure 5-7: Chiller operation between (VCC vs. VCC+CWS)
(Large Hotel in Boston)

5.6.1 Dispatch for a CWS tank

Figure 5-7 demonstrates that, in a Large Hotel in Boston, a CWS tank is only used when high cooling demand is expected; conversely, during days with low cooling demand, the CWS is used very little or not at all. This can be explained by the fact that there is no time-of-use pricing in Boston and thus, the only incentive for using the CWS is peak shaving. The increased utilization of the CWS tank can be credited to the fact that there is a significant difference between peak and off-peak energy charges for electricity. Thus, savings are generated by generating chilled water for storage with off-peak electricity prices and then discharging the cold water when peak energy charges apply.

Due to the time-of-use and demand charges, we would have expected that more savings could be achieved in San Francisco than in Boston. However, higher savings are achieved in Boston with CWS. This can be explained by the fact that high demand charges have been applied for monthly peaks and cooling demand is the main contributor to the monthly peaks in Boston. In addition, the size of the VCC in a large hotel in Boston is decreased by 220kW compared to 130kW in San Francisco. In San Francisco the cooling demand contributes less to the total peak

and cooling comprises a smaller share of the total costs; thus, installing a CWS tank has less of an impact on the total costs in San Francisco.

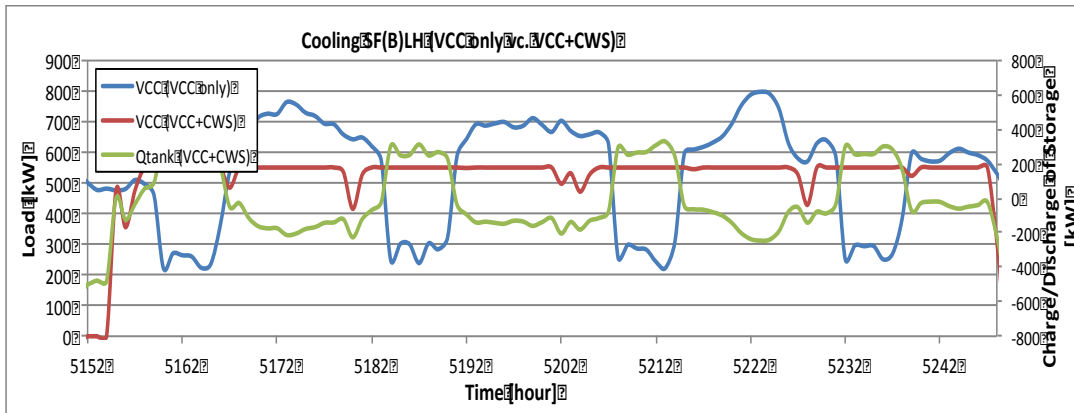


Figure 5-8: Chiller operation (VCC vs. VCC+CWS)
(Large Hotel in Boston – with San Francisco utility pricing)

Figure 5-11 illustrates the share of monthly peak demand contributed by the electric driven vapor compression chiller for a large hotel in Boston and San Francisco. The VCC contribution is significant in Boston, especially during summer when demand charges are increased from \$20/kW to \$28/kW. In the figures below (Figure 5-9 and Figure 5-11) power purchases from the grid are presented, for different system configurations, for a two-day period (a large hotel in Boston and a large hotel in San Francisco).

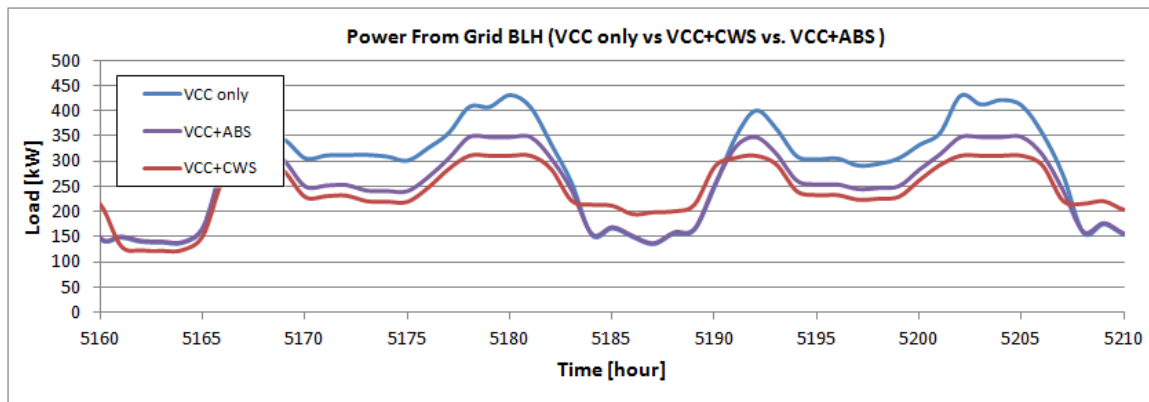


Figure 5-9: Two-day power needs profile of a large hotel in Boston
(VCC only vs. VCC+ABS vs. VCC+CWS)

The installation of additional equipment alters the demand profile of a building differently at the presence of different utility pricing structures. At locations with high demand

charges, such as Boston, the main goal is to shave the monthly peak. The addition of absorption chillers results in shifting the power consumption profile of the VCC down peak-hours, while the load during off-hours remains the same.

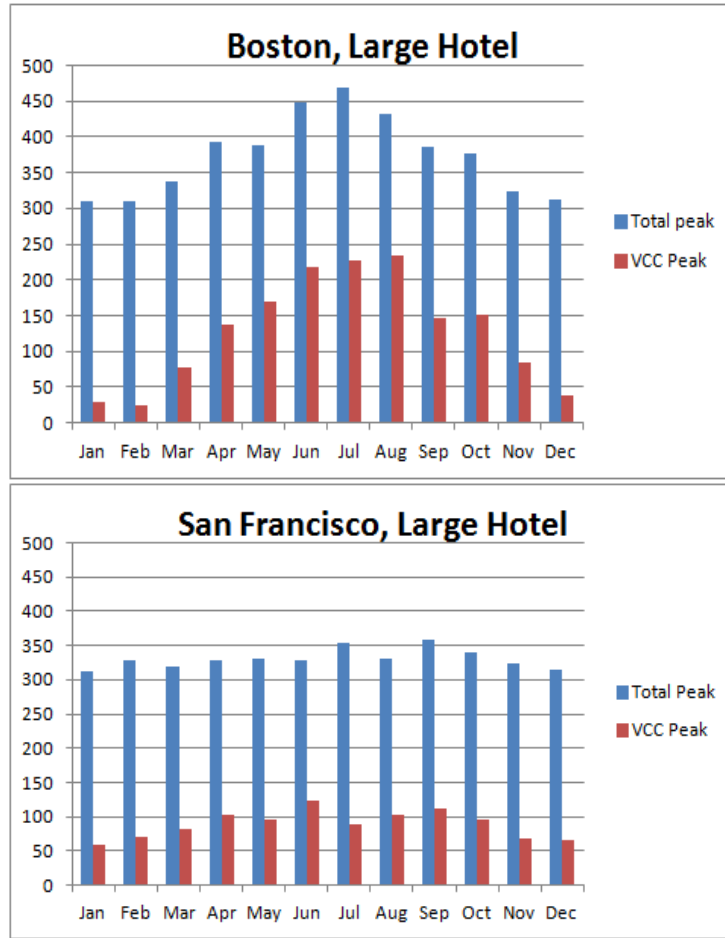


Figure 5-10: Share of VCC electricity the monthly peaks

The addition of CWS results in a further shift of the power demand of the VCC, compared to a VCC+ABS system, and an increase of power consumption during off-peak demand (load shifting). CWS tends to slightly “smoothens” the power demand profile of the building over the course of a day. For a location with time-of-use pricing, like San Francisco, peak reduction is not a priority; rather, the priority is to reduce demand during peak energy charges. The installation of an absorption chiller shifts the whole power demand of the VCC down, where in Boston only the daily peak is shifted down. A CWS tank in San Francisco performs load shifting and peak reduction has low priority, discharge of the CWS tank takes place during peak-energy charges (between the two peaks in Figure 5-11) and no or little

discharge during demand peaks (the highest tips of the load profile on Figure 5-11). Peak shaving in San Francisco (average reduction in monthly peaks by -9%) is less relevant compared with a large hotel in Boston (average reduction in monthly peaks by -14%).

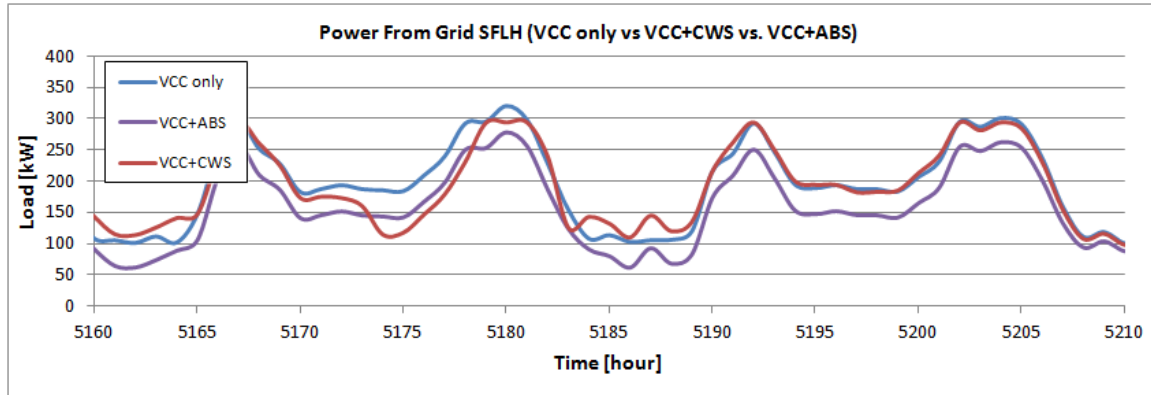


Figure 5-11: Two-day power needs profile of a large hotel in San Francisco (VCC only vs. VCC+ABS vs. VCC+CWS)

Table 5-6: Summary of results

System Configuration	Location	Building Type	Payback Time [years]	Change in Total Annual Savings [%]	Change in CO ₂ Emissions [%]
VCC+ABS	Boston	Hotel	7.2	-1.53	0.48
	Boston	Office	7.7	-1.33	0.47
	San Fran.	Hotel	4.3	-3.08	5.63
	San Fran.	Office	7.8	-0.68	5.64
VCC+CWS	Boston	Hotel	0	-10.83	-2.63
	Boston	Office	0	-16.08	-1.54
	San Fran.	Hotel	0	-7.08	-2.31
	San Fran.	Office	0	-10.74	-3.93

5.7 Summary of Results

The chiller COP and CO₂ tax have small impacts on the design and dispatch; however, the impact on the total annual cost is significant. Investigation of individual technologies shows that a CWS tank is the choice of DG promising negative payback times and significant reductions in total annual costs of meeting (7-16%) the energy needs of buildings.

CHAPTER 6

CONCLUSIONS

The model is capable of finding the design and dispatch employing cold thermal storage tanks for annual hourly data was implemented to study the technical and economic viability in commercial building applications. The model includes the following technologies: auxiliary boiler, absorption and vapor compression chillers with fixed COP values, and cold thermal energy storage. The primary objective of this study is to identify attractive system integration concepts for combinations of DG technologies, building profiles, and utility pricing structures that generate savings for a building operator. The model created is based on the work done by Pruitt et al. 2012 [47].

6.1 Major Findings

A sensitivity analysis is performed to characterize the effects of a set of chosen parameters (see Table 4-2) to the design, dispatch and economics of an onsite building energy system. Secondly, individual technologies are investigated to find which one of them will result in highest savings and/or shortest payback periods for a building operator.

6.1.1 Effect of DER technology efficiency performance

- COP values of the chillers and a tax on CO₂ emissions have only a small impact on the design, dispatch but a significant impact on the total annual costs.

6.1.2 Effect of cold thermal storage

- Investigation of different DG technologies indicates that the most beneficial DG technology is a CWS tank. The installation of CWS tank reduces the overall installed cost of the cooling system resulting in a negative payback time for the new system, plus, the annual savings are significant (total savings of in the 7 to 16% compared to the baseline case, see Table 5-5). Considering the above results a building owner should consider the installation of a CWS on-site.
- Comparison of building types revealed that a CWS tank has higher savings potential in a medium sized office; a strong incentive is due to significant difference between daily peak and baseload.

6.1.3 Effect of system configuration

- The addition of natural gas fired absorption chillers to a cooling system consisting of VCCs results in savings in the 1% range. A mix of vapor compression and absorption chillers increases the total capital cost of the cooling equipment, however, the simple payback time, even with marginal savings, is less than 8 years for locations and building types investigated.

6.2 Future Work

There are several aspects and improvements of the model that can be pursued for future work. For example, a variable COP value of the chillers could be adopted. A COP is a function of part load ratio and the wet bulb temperature promote generating and storing more chilled water during night time as lower wet bulb temperatures improve the COP of both the VC and the absorption chiller. Higher COP values during off-peak hours can promote the installation of a larger CWS tank.

Building clusters can be investigated instead of a single building. DG can benefit from building clusters because a larger devices can be installed and benefit from economy of scale. In addition, building clusters can also promote “smoothing” of load profiles; a smoother load

profile can improve capacity factors of different technologies as well as improve the COP values of chillers. A “smoothened” load profile is likely to reduce the benefit of CWS, as one of the main drives for a CWS is the difference between the daily peak and baseload values. However, a large difference between daily peak and minimum is only one of the drivers for CWS and there are several other, the most relevant ones are: difference between peak and off-peak electricity pricing, demand charges and reduced size of cooling equipment (reduced installed cost resulting in negative payback times). Additionally, the thermal capacity of the building should be taken into account as pre-cooling of the building can reduce cooling loads during peak electricity price periods.

The installed cost of many devices is a function of the installed capacity, thus, the cost per installed unit should be a function of the total installed capacity. The specific cost (\$/kW, \$/ton_{refr}) of small devices, such as absorption chillers, are considerably more expensive than larger absorption chillers.

Limits on ramp rates of the chillers should be applied as has been done with the SOFC in the study at hand. However, in this study we only consider hourly load data, making even steep ramp rates seem more reasonable than they really are. In order to realistically evaluate the limitations of ramp rates to the dispatch of VCC, absorption chillers and SOFC, the time-step in the model needs to be reduced to below one hour.

Preliminary results show that a the waste heat of a CHP-SOFC can be fully utilized in a large hotel and medium sized office in Boston and San Francisco, making the economic viability of CCHP energy systems questionable (little additional economic gain). The only exception is a medium sized office located in San Francisco, where the upgrades from a CHP to a CCHP can double the waste heat utilization. Preliminary results also indicate that in addition to retrofitting the cooling system of the building, the heating system (auxiliary boiler) should be replaced with a new one (with added installed cost for the auxiliary boiler). By doing so, there is more incentive for the installation of a HWS tank. We expect that the HWS tank will decrease the size of the hot water boiler similar to the way in which the CWS tank decreased the size of chillers.

REFERENCES CITED

- [1] 14Group Engineering, <http://www.group14eng.com/>. Personal communication with Brian Graham - January 2013
- [2] Adjiman C. and C. Floudas. “ α BB algorithm. Encyclopedia of Optimization, 1: 61–73, 2008.
- [3] Al-Sulaiman F.A., F. Hamdullahpur and I. Dincer. “Performance Comparison of Three Trigeration Systems Using Rankine Cycles.” *Energy* 36 (2011): 5741-5754.
- [4] Alanne K., N. Söderholm, K. Siren and I. Beausoleil-Morrison. “Techno-economic assessment and optimization of Stirling engine micro-cogeneration systems in residential buildings.” *Energy Conversion and Management* 51 (2010): 2635-2646.
- [5] Arcuri P., G. Florio and P. Fragiaco. “A Mixed Integer Programming Model for Optimal Design of Trigeration in a Hospital Complex.” *Energy* 32 (2007): 1430-1447.
- [6] ASHRAE. “Application Guide for Absorption Cooling/Refrigeration Using Recovered Heat.” *ASHRAE* (1995)
- [7] ASHRAE. “Design Guide for Cool Thermal Storage.” *ASHRAE* (1993)
- [8] ASHRAE. “HVAC Systems and Equipment – Cooling Towers.” *ASHRAE* (2008)
- [9] Bompardi E., R. Napoli, B. Wan and G. Orsello. “Economics Evaluation of a 5 kW SOFC Power System.” *International Journal of Hydrogen Energy* 33 (2008): 3243-3247.
- [10] Braun R.J. “Techno-economic optimal design of SOFC systems for residential micro-combined heat and power applications in the U.S.” *ASME Journal of Fuel Cell Science and Technology* 7 (2010): 1-15.
- [11] Braun R.J. “Techno-Economic Optimal Design of Solid Oxide Fuel Cell Systems for Micro-Combined Heat and Power Applications in the U.S.” *Journal of Fuel Cell Science and Technology* 7 (June 2010): 031018-2.
- [12] Buildings Energy Data Book 2012, U.S. Department of Energy, accessed December 2012, <http://buildingsdatabook.eren.doe.gov>
- [13] Carbon Tax Center 2012, accessed March 2012, <http://www.carbontax.org>
- [14] Center for Sustainable Energy, California “2013 Self-Generation Incentive Program HANDBOOK.” (2013)
- [15] Chicco G. and P. Mancarella. “Generation primary energy savings evaluation for energy planning and policy development.” *Energy Policy* 35 (2007): 6132-6144.
- [16] Clausen J. “Subdivision, sampling, and Initialization Strategies for Simplicial Branch and Bound in Global Optimization.” *Computers and Mathematics with Applications* 44 (2002): 943-955.
- [17] Deng J., R.Z. Wang and G.Y. Han. “A review of thermally activated cooling technologies for combined cooling, heating and power systems.” *Progress in Energy and Combustion Science* 37 (2011): 172-203.
- [18] Deutschmann O. “Solid Oxide Fuel Cells (SOFC): Direct internal reforming.” *Karlsruhe Institute of Technology*
- [19] Duffie J.A. and W.A. Beckman. “Solar Engineering of Thermal Processes. 2nd Edition” *Wiley Interscience* (1991)
- [20] Ehyaei M.A., A. Mozafari, A. Ahmadi, P. Esmaili, M. Shayesteh, M. Sarkhosh and I. Dincer. “Potential Use of Cold Thermal Energy Storage Systems for Better Efficiency and Cost Effectiveness.” *Energy and Buildings* 42 (2010): 2296-2303.

- [21] Eicker U. and D. Pietruschka. "Design and performance of Solar Powered Absorption Cooling Systems in Office Buildings." *Computers and Chemical Engineering* 48 (2013): 40-47.
- [22] Environmental Protection Agency 2013, accessed April 2013, <http://www.epa.gov/>
- [23] Gumerman, E.Z., R.R. Bharvirkar, K.H. LaCommare and C. Marnay. "Evaluation Framework and Tools for Distributed Energy Resources." *Ernest Orlando Lawrence Berkeley National Laboratory*, 2003.
- [24] Haeseldonckx D., L. Peeters, L. Helsen and W. D'haeseleer. "The Impact of Thermal Storage on The Operational Behaviour of Residential CHP Facilities and The Overall CO₂ Emissions." *Renewable and Sustainable Energy Reviews* 11 (2007): 1227-1243.
- [25] Homer Energy 2013, accessed November 2012, <http://www.homerenergy.com/>
- [26] Ievers S. and W. Lin. "Numerical simulation of three-dimensional flow dynamics in a hot water storage tank." *Applied Energy* 86 (2009): 2604-2614.
- [27] Jiang-Jiang W., Z. Chung-Fa and J. You-Yin. "Multi-criteria Analysis of Combined Cooling, Heating and Power Systems in Different Climate Zones in China." *Applied Energy* 87 (2010): 1247-1259.
- [28] Jing Y-Y., H. Bai and J-J. Wang. "A Fuzzy Multi-criteria Decision-Making Model for CCHP Systems Driven by Different Energy Sources." *Energy Policy* 42 (2012): 286-296.
- [29] Kavvadias K.C. and Z.B. Maroulis. "Multi-objective optimization of a trigeneration plant." *Energy Policy* 38 (2010): 945-954.
- [30] Kavvadias K.C., A.P. Tosios and Z.B. Maroulis. "Design of a combined heating, cooling and power system: Sizing, operation strategy selection and parametric analysis." *Energy Conversion and Management* 51 (2010): 833-845.
- [31] Kintner-Meyer M. and A.F. Emery. "Optimal Control of an HVAC System Using Cold Storage and Building Thermal Capacitance." *Energy and Building* 23 (1995): 19-31.
- [32] LeMar P. "Integrated Energy Systems (IES) for Buildings: A Market Assessment." *Resource Dynamics Corporation* (September 2002): ORN/SUB/409200.
- [33] Li Y., X. Wang, D. Li and Y. Ding. "A Trigeneration System Based on Compressed Air and Thermal Energy Storage." *Applied Energy* 99 (2012): 316-323.
- [34] Mago P.J. and A.K. Hueffed. "Evaluation of a Turbine Driven CCHP System for Large Office Buildings Under Different Operating Strategies." *Energy and Buildings* 42 (2010): 1628-1636.
- [35] Manfren M., P. Caputo and G. Costa. "Paradigm Shift in Urban Energy Systems Through Distributed Generation: Methods and Models." *Applied Energy* 88 (2011): 1032-1048.
- [36] Margalef P. and S. Samuelsen. "Integration of a molten carbonate fuel cell with a direct exhaust absorption chiller." *Journal of Power Sources* 195 (2010): 5674-5685.
- [37] Maribu K.M., R.M. Firestone, C. Marnay and A.S. Siddiqui. "Distributed Energy Resources Market Diffusion Model." *Energy Policy* 35 (2007): 4471-4484.
- [38] MassSAVE 2013, accessed May 2013, <http://www.masssave.com>
- [39] Nexant Inc. "Equipment Design and Cost Estimation for Small Modular Biomass Systems, Synthesis Gas Cleanup, and Oxygen Separation equipment. Task 1: Cost Estimation of Small Modular Systems." *Subcontract Report NREL/SR-510-39943*, May 2005, San Francisco, CA
- [40] NSTAR 2013, accessed April 2013, <http://www.nstar.com/>
- [41] O'Hayre R., S-W., W. Colella and F.B. Prinz. "Fuel Cell Fundamentals" *Wiley* (2009)

- [42] Onovwiona, H.I., and V.I. Ugursal. "Residential Cogeneration Systems: Review of the Current Technology." *Renewable and Sustainable Energy Reviews* 10 (2006): 389-431.
- [43] Pacific Gas and Electricity 2013, accessed March 2013, <http://www.pge.com/>
- [44] Pecas Lopes, J.A., N. Hatziargyriou, J. Mutale, O. Djapic and N. Jenkins. "Integrating Distributed Generation Into Electric Power Systems: A Review of Drivers, Challenges and Opportunities." *Electric Power Systems Research* 77 (2007): 1189-1203.
- [45] Pinel P., C.A. Cruickshank, I. Beausoleil-Morrison and A. Wills. "A review of available methods for seasonal storage of solar thermal energy in residential applications." *Renewable and Sustainable Energy Reviews* 15 (2011): 3341-3359.
- [46] Pirkandi J., M. Ghassemi, M.H. Hamedi and R. Mohammadi. "Electrochemical and thermodynamic modeling of a CHP system using tubular solid oxide fuel cell (SOFC-CHP)." *Journal of Cleaner Production* 29-30 (2012): 151-162.
- [47] Pruitt, K. A. (2012). *A Mixed-Integer Nonlinear Program for The Optimal Design and Dispatch of Fuel Cell-Based Distributed Generation Systems*. Division of Economics & Business. Colorado School of Mines. Golden, CO.
- [48] RETScreen International 2013, accessed November 2012, <http://www.etscreen.net/>
- [49] Sayyaadi H. "Multi-Objective Approach in Thermoenvionomic Optimization of a Benchmark Cogeneration System." *Applied Energy* 86 (2009): 867-879.
- [50] Siddiqui A.S., C. Marnay, O. Bailey and K.H. LaCommare. "Optimal Selection of On-Site Generation with Combined Heat and Power Applications." *Ernest Orlando Lawrence National Laboratory* (November 2004): LBNL 56774.
- [51] Smith A.D., P.J. Mago and N. Fumo. "Benefits of Thermal Energy Storage Option Combined CHP System for Different Commercial Building Types." *Sustainable Energy Technologies and Assessment* 1 (2013): 3-12.
- [52] Southern California Edison 2013, accessed March 2012, <http://www.sce.com/>
- [53] Southern California Gas Company 2013, accessed March 2012, <http://www.socalgas.com/>
- [54] Stuhlenmiller T. and R. Koenigsdorff. "Optimum Thermal Storage Sizing in Building Services Engineering as a Contribution to Virtual Power Plants." *Journal of Building Performance Simulation* 3-1 (2010): 17-31.
- [55] Tan, C.W., T.C. Green and C.A. Hernandez-Azamburo. "A Stochastic method for Battery Sizing Uninterruptible-Power and Demand Shift Capabilities in PV (Photovoltaic) Systems." *Energy* 35 (2010): 5082-5092.
- [56] Thornton, A. and C.R. Monroy. "Distributed Power Generation in the United States." *Renewable and Sustainable Energy Reviews* 15 (2011): 4809-4817.
- [57] Tichi S.G., M.M. Ardehali and M.E. Nazari. "Examination of Energy Price Policies in Iran for Optimal Configuration of CHP and CCHP Systems Based on Particle Swarm Optimization Algorithm." *Energ Policy* 38 (2010): 6240-6250.
- [58] Trendewicz A.A. and R.J. Braun. "Techno-economic analysis of solid oxide fuel cell-based combined heat and power systems for biogas utilization at wastewater treatment facilities." *Journal of Power Sources* 233 (2013): 380-393.
- [59] Trigenation 2013, accessed March 2013, <http://www.trigenation.com>
- [60] Vetterli J. and M. Benz. "Cost-optimal Design of an Ice-storage Cooling System Using Mixed-integer Linear Programming Techniques Under Various Electricity Tariff Schemes." *Energy and buildings* 49 (2012): 226-234.

- [61] Wagner T., T. Rosfjord and A. Morrow. "Report for The Field Scale Test and Verification of a PureComfort® 240M Combined Heat and Power System, at the Ritz Carlton, San Francisco." *Computers and Chemical Engineering* 48 (2013): 40-47.
- [62] Weber C., F. Marechal, D. Favrat and S. Kraines. "Optimization of an SOFC-based Decentralized Polygeneration System for Providing Energy Services in an Office Building in Tokyo." *Applied Thermal Engineering* 26 (2006): 1409-1419.
- [63] Wikipedia. 2013, accessed August 2013, <http://www.wikipedia.com>
- [64] Wu J-Y., J-l. Wang and S. Li. "Multi-objective Optimal Operation Strategy Study of Micro-CCHP System." *Energy* 48 (2012): 472-483.
- [65] Yazaki Energy Systems, Inc. 2013, accessed March 2013, <http://www.yazakienergy.com>
- [66] Yu Z., J. Han and X. Cao. "Investigation on Performance of an Integrated Solid Oxide Fuel Cell and Absorption Chiller Tri-generation System." *International Journal of Hydrogen Energy* 36 (2011): 12561-12573.
- [67] Zhang C., M. Yang, M. Lu, Y. Shan and J. Zhu. "Experimental Research on LiBr Refrigeration – Heat Pump System Applied." *Applied Thermal Engineering* 31 (2011): 3706-3712.
- [68] Zhou Z., P. Liu, Z. Li, E.N. Pistikopoulos and M.C. Georgiadis. "Impacts of Equipment Off-Design Characteristics on The Optimal design and Operation of Combined Cooling, Heating and Power Systems." *Computers and Chemical Engineering* 48 (2013): 40-47.
- [69] Zink F., X. Lu and L. Schaefer. "A solid oxide fuel cell system for buildings." *Energy Conversion and Management* 48 (2007): 809-818.
- [70] Liu, C. (2012). *Model Predictive Optimal Control for Active and Passive Thermal Energy Storage of Multi-Zone Buildings*. Department of engineering. Colorado School of Mines. Golden, CO.